 https://doi.org/10.22201/fc.25942158e.2022.2.422

POSTNATAL OSSIFICATION PATTERN AND HETEROCHRONIES IN ANDEAN GYMNOPHTHALMOIDEA LIZARDS

PATRÓN DE OSIFICACIÓN POSTNATAL Y HETEROCRONÍAS EN LAS LAGARTIJAS ANDINAS DE GYMNOPHTHALMOIDEA

Torres-Vásquez Itza Hinumaru[1], Jerez Adriana[1*] & Arenas-Rodríguez Angélica[2]

[1]*Laboratorio de Ecología Evolutiva. Departamento de Biología, Facultad de Ciencias, Universidad Nacional de Colombia, Sede Bogotá. Bogotá. Colombia.*

[2]*Laboratorio de Sistemática y Biogeografía de Vertebrados. Departamento de Biología, Facultad de Ciencias, Unidad de Ecología y Sistemática-UNESIS, Pontificia Universidad Javeriana, Sede Bogotá. Bogotá. Colombia.*

**Correspondence: arjerezm@unal.edu.co*

Received: 2022-02-16. **Accepted**: 2022-05-05. **Published:** 2022-05-26.

Editor: Marissa Fabrezzi, Argentina.

Resumen.— Gymnophthalmoidea es un clado compuesto por las familias Alopoglossidae, Teiidae y Gymnophthalmidae. La distribución geográfica de tierras bajas a altoandinas, la existencia de especies pequeñas y muy grandes y la evolución de formas con alargamiento corporal y reducción de extremidades hacen de este grupo un modelo único para explorar el desarrollo del esqueleto. Los estudios del desarrollo postembrionario no solo constituyen los cambios en la forma del esqueleto, sino también el patrón de osificación, que constituye una fuente de información filogenética. Por lo tanto, describimos el patrón de osificación del esqueleto de algunas especies de Gymnophthalmidae (*Anadia bogotensis, Riama striata*) y Alopoglossidae (*Alopoglossus bicolor*) y comparamos con otras especies en Gymnophthalmoidea. Además, analizamos los eventos heterocrónicos incluyendo Alopoglossidae, Teiidae y Gymnophthalmidae. Encontramos que Gymnophthalmoidea comparte características del patrón de osificación con Squamata en el cráneo y las extremidades. Un evento heterocrónico es compartido por Gymnophthalmidae, en el cual, la epífisis del radio desarrolla centros de osificación más tarde que las epífisis del húmero, ulna, metacarpo, fémur y el carpo. En conclusión, *A. bogotensis, R. striata* y *B. bicolor* comparten características que las separan de *A. bicolor*, indicando diferencias filogenéticas, las cuales son evidentes en un evento heterocrónico en el patrón de osificación del esqueleto. Entoces, los estudios descriptivos y comparativos del esqueleto aportan información de valor filogenético importante en la comprensión de la evolución de los Gymnophthalmoidea y lagartos escamados en general.

Palabras clave.— Alopoglossidae, Gymnophthalmidae, desarrollo postembrionario, esqueleto, ontogenia.

Abstract.— Gymnophthalmoidea is a clade composed of the families Alopoglossidae, Teiidae and Gymnophthalmidae. Their geographical distribution, from lowlands to highlands in the Andes, with small and very large species, and species with body elongation and limb reduction, makes this group a model to explore the development of skeleton. The pattern of ossification during postembryonic development is a source of phylogenetic information. For this reason, we described the ossification pattern of some species of Gymnophthalmidae (*Anadia bogotensis, Riama striata*) and Alopoglossidae (*Alopoglossus bicolor*) and compared it with other species in Gymnophthalmoidea. In addition, we analyzed whether the events of the ossification pattern constitute heterochronies of phylogenetic value between Alopoglossidae, Teiidae and Gymnophthalmidae. We found that Gymnophthalmoidea shares characteristics of the ossification pattern with Squamata in the skull and limbs. A heterochronic event was reported for Gymnophthalmidae, in which the development of secondary centers of ossification in radial epiphyseal cartilages occurs later than ossifications in the humeral, ulnar, metacarpal and femoral epiphyseal cartilages, and carpus. In conclusion, *A. bogotensis,*

R. striata and *B. bicolor* share characteristics different from *A. bicolor,* indicating phylogenetic differences, which was evident for a heterochronic event reported in this study for Gymnophthalmoidea. Therefore, skeleton studies provide relevant phylogenetic information to understand the evolution of Squamata.

Keywords.– Alopoglossidae, Gymnophthalmidae, ontogeny, postembryonic development, skeleton.

INTRODUCTION

Gymnophthalmoidea (Goicoechea et al., 2016) is a clade composed of three families distributed in the Neotropics (Fig. 1). Teiidae (172 species) is a conspicuous clade in the lowlands, while Alopoglossidae (29 species) and Gymnophthalmidae (270 species) spread across the Andean highlands (Uetz et al., 2021). Evolutionary analyses established that the clade informally known as microteids, previously considered a part of Teiidae, is a different evolutionary unit, now accepted as Alopoglossidae and Gymnophthalmidae (Presch, 1980; 1983; Estes et al., 1988; Hoyos, 1998; Pellegrino et al., 2001; Castoe et al., 2004; Goicoechea et al., 2016).

In this clade, the species vary between the lacertiform and the serpentiform body plans observed in Squamata. The serpentiform body plan has been evolved with changes in head size, body elongation (more than 27 vertebrae) and limb reduction (Gans, 1975; Presch, 1975; Pellegrino et al., 2001; Wiens & Slingluff, 2001; Grizante et al., 2012). The lacertiform body plan is observed in Teiidae and Alopoglossid species, with robust limbs, and without body elongation, which it means 26 vertebrae (Presch, 1975; Pellegrino et al., 2001; Wiens & Slingluff, 2001; Grizante et al., 2012). The serpentiform body plan is observed in Gymnopthalmidae with slim trunk, limb reduction, and very evident body elongation with more than 30 vertebrae (Presch, 1975; Pellegrino et al., 2001; Wiens & Slingluff, 2001; Grizante et al., 2012). Between lacertiform and serpentiform body plans there are also species with an intermedius morphology in Gymnopthalmidae, which exhibit 27 to 29 vertebrae (Presch, 1975; Pellegrino et al., 2001; Grizante et al., 2012).

The hypothesis from the molecular perspective yields new systematic arrangements, which constitute an invaluable basis

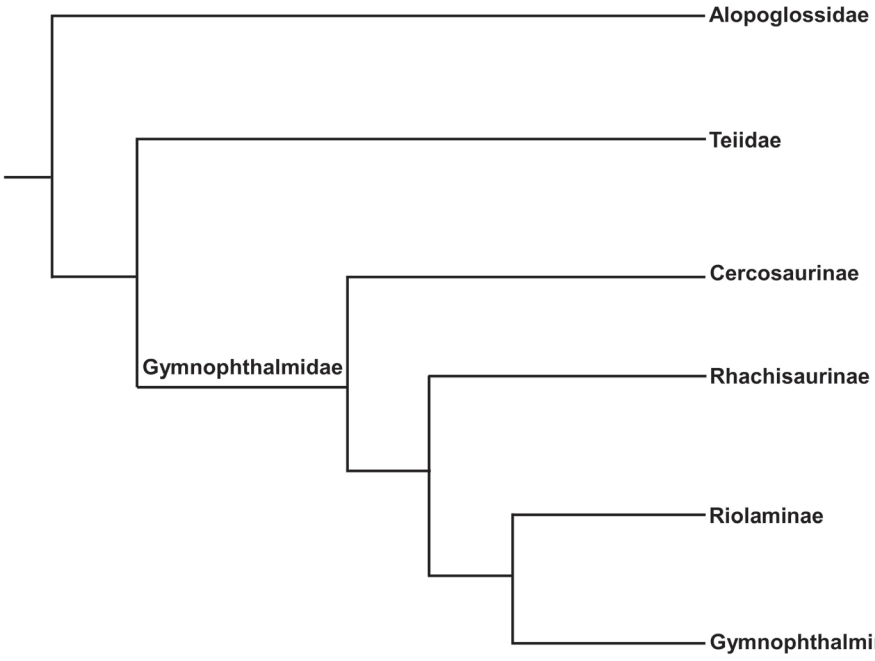

Figura 1. Relaciones filogenéticas de las familias de Gymnopthalmoidea (Squamata), con base en Goicoechea (2016).

Figure 1. Phylogenetic relationships within Gymnophthalmoidea (Squamata), following Goicoechea (2016).

for the analysis of morphological changes in the skeleton between body plans in an evolutionary context. Hernández-Morales et al. (2019) analyzed *Alopoglossus vallensis* and proposed characters for Alopoglossidae, highlighting the need for descriptive studies. In Gymnophthalmidae, different morphological patterns related to the evolution of the skeleton have been analyzed in adults. Pellegrino et al. (2001) proposed five possible independent origins for the evolution of the serpentiform body plan, which include skull reduction, limb reduction or loss, and body elongation. Kohlsdorf & Wagner (2006) found in *Bachia*, that the pattern of reduction involves the re-evolution of digits. Barros et al., (2011) observed that ecological factors such as microhabitat use are determinant in the evolution of skull shape in burrowing adult species in Gymnophthalmidae.

Descriptive anatomical studies of embryonic (Arias & Lobo, 2006; Hernández-Jaimes et al., 2012; Roscito & Rodrigues, 2012a, b; Lungman et al., 2019; Jerez et al., 2020) and postembryonic skeletal development are scarce in Gymnophthalmoidea, despite its wide distribution and diversity in the American continent. Postnatal development of the skull and appendicular skeleton has been described in the serpentiform gymnophthalmid *Bachia bicolor* (Tarazona et al., 2008; Jerez & Tarazona, 2009), while in the lacertiform gymnophthalmid *Potamites ecpleopus* some changes were described during the postnatal skull development (Bell et al., 2003). In the lacertiform teiids, the ossification of the skeleton at hatching of *Aspidoscelis tigris* was analyzed and compared to other squamates (Maisano, 2001), and the pattern of ossification in embryonic development was described for *Tupinambis merianae* and *Tupinambis rufescens* (Arias & Lobo, 2006). Finally, Jerez et al. (2020) compared embryonic development between gimnoftalmids, alopoglossids and teiids, and they proposed that peramorphosis is responsible for body elongation and paedomorphosis for limb reduction, in the evolution of serpentiform species in this clade.

The postnatal ossification pattern from a descriptive and comparative perspective provides useful phylogenetic information, but also allows one to establish whether heterochronic changes are related to morphological patterns and to analyze the evolutionary change (Weisbecker & Nilsson, 2008; Koyabu & Son, 2014). This is relevant in Gymnophthalmoidea in which several species have evolved between large and small sizes, and exhibit transformations between the lacertiform and serpentiform body plan with body elongation and reductions in the skull and limbs (Presch, 1975; Greer, 1991; Pellegrino et al., 2001; Grizante et al., 2012). Hence, the goals of this work are to describe the ossification pattern in *Anadia bogotensis*, to compare it with two gymnophthalmids (*Riama striata* and *Bachia bicolor*) and an alopoglossid (*Alopoglossus bicolor*), and to determine if heterochronic events of phylogenetic importance can be found in Gymnophthalmoidea based on the ossification pattern of the skeleton.

MATERIALS AND METHODS

Specimens

The specimens of *Anadia bogotensis* and *Riama striata* (Gymnophthalmidae) were obtained from the Colección Herpetológica of the Instituto de Ciencias Naturales (ICN) of the Universidad Nacional de Colombia, Sede Bogotá, including only specimens from the same population (Appendix 1). For *Allopoglossus bicolor* (Alopoglossidae), we analyzed cleared and stained specimens deposited in the Colección Herpetológica of the Universidad Industrial de Santander (UIS, Bucaramanga, Colombia, Appendix 1). The developmental stage was determined according to the snout-vent length (SVL) and reproductive biology data, considering the adult stage from the moment that sexual maturity is reached. The sex was not considered as a source of variation due to the small sample size.

In the case of *A. bogotensis*, neonatal size varies from 20 to 28 mm SVL, and sexual maturity is reached at 40 mm SVL (Jerez & Calderón-Espinosa, 2014). The series was obtained from twelve specimens (Appendix 1): three neonates (SVL: 22.33 mm, 23.86 mm, and 26.46 mm); two juveniles (SVL: 31.36 mm and 36.55 mm); and seven adults (SVL: 42.53 mm, 48.63 mm, 50 mm, 50.36 mm, 52.6 mm, 58.23 mm, and 62.67 mm). For *R. striata* the neonatal size is 28 mm and sexual maturity is reached at 46 mm SVL in females and 50 mm SVL in males (Méndez-Galeano & Pinto-Erazo, 2018). The ontogenetic series was obtained from six individuals (Appendix 1): two neonates (SVL: 28 mm and 28.85 mm); a single juvenile (SVL: 38.7 mm); and three adults (SVL: 52.63 mm, 58.02 mm, and 66.2 mm). The specimens were cleared and bone and cartilage differentially stained with Alcian Blue and Alizarin, following the protocol proposed by Wassersug (1976). For *A. bicolor* (Alopoglossidae), neonatal size is 23.8 mm SVL, and females and males reach sexual maturity between 46.2 mm and 44 mm SVL, respectively (Ramos-Pallares et al., 2010). According to the available collection material, the series included (Appendix 1): two neonates, one complete (SVL: 23.8 mm, cranium and postcranium) and one without a skull (20.2 mm BL: body length); three juveniles, one complete (SVL: 30.24 mm) and two without limbs (SVL: 43.88 mm and 44.28 mm); and seven adults, three complete (SVL: 50.24 mm, 51.92 mm, and 56.24 mm), two without limbs (SVL: 51.46 mm and 60.28 mm) and two without a skull (SVL: 54.4 mm and 55.12 mm).

Pattern of ossification

We described the pattern of ossification for the gimnoftalmids *Anadia bogotensis* and *Riama striata* and the alopoglossid *Allopoglossus bicolor* during postembryonic development. The nomenclature of bone elements and ossification pattern description of the skull is based on Bellairs & Kamal (1981) and Evans (2008), and the appendicular elements are based on Fabrezi et al. (2007) and Krause (1989). The ossification patterns are based on Maisano (2002a, b, c), including the ossification of epiphyseal cartilages from secondary centers (SCs), the basipodial element from ossification centers (OCs), and the differentiation of apophyseal ossifications. The epiphyseal cartilages are ossified and fusing with the diaphyses when the sutures are present, and the fusion between epiphyses and diaphyses is complete when the sutures disappear. Finally, we followed Jerez et al. (2010) to identify sesamoids. The skeletal ossification pattern of the most complete series of *A. bogotensis* were described from neonates to the largest adult in the population. Then, differences in the ossification pattern of *R. striata* and *A. bicolor* were contrasted (with the ones of *A. bogotensis*).

Ossification sequences

For interspecific comparisons of ossification sequences in postembryonic development we made a rank analysis (Nunn & Smith, 1998; Smith, 2001; Germain & Laurin, 2009; Keyte & Smith, 2010). The ossification sequences were established for *A. bogotensis, R. striata* and *A. bicolor* on the pattern of ossification for each species. We included the gimnoftalmid *Bachia bicolor* following the literature (Tarazona et al., 2008; Jerez & Tarazona, 2009).

For the rank analysis, the following events in the skull were taken into account. For the dermatocranium, the presence and closure of the frontoparietal fontanelle. For the basicranium, initially, the ossification of all elements of basicranium but separated by synchondroses; then, the fusion of bony elements of the basicranium, with the presence of basicranial sutures; and finally, the complete fusion of all bony elements of the braincase, such that the sutures are no longer discernible. Finally, the presence and closure of the basicranial fenestra between basioccipital and sphenoid.

For the limbs, we considered the following events. In the epiphyseal cartilages, initially, the appearance of SCs; then, the complete ossification of epiphyseal cartilages but with suture with the diaphyses; and finally, the complete fusion between epiphyses and diaphyses, when the sutures are no longer discernible; in the case of the phalanges, only the proximal phalanges were included. For the carpal and tarsal elements, initially the presence of OCs and later their complete ossification. For the astragalus and calcaneum, the presence of OCs, the fusion with perceptible suture, and their complete fusion.

In the rank analysis, the events that ossify at the same time in the sequence are denominated as the same rank in the ossification sequence (Nunn & Smith, 1998; Smith, 2001; Germain & Laurin, 2009; Keyte & Smith, 2010). We identified which ranks present greater interspecific variation within the sequences through a rank analysis using a standardized matrix (Germain & Laurin, 2009) to homogenize events into sequences.

Heterochronic analysis

Finally, to identify heterochronic events within Gymnophthalmoidea, we used the pattern of ossification of neonates of alopoglossid *A. bicolor,* the gimnoftalmids *A. bogotensis, R. striata,* and *B. bicolor*. We included the gimnoftalmid *Potamites ecpleopus* and the teiid *Aspidocelis tigris* following Maisano (2001). We performed Parsimov analysis and based genetic inference analysis (Nunn & Smith, 1998; Smith, 2001; Jeffery et al., 2002; Smith, 2001; Keyte & Smith, 2010; Hautier et al., 2013). A pruned phylogenetic tree with the species analyzed was generated from the phylogeny established by Goicoechea et al. (2016).

Then, heterochronic events were identified using the neonatal ossification state for three families of Gymnophthalmoidea (Alopoglossidae, Teiidae and Gymnophthalmidae). For this analysis the following ossification events were included, for the skull: a) the fusion with suture between supraoccipital and exoccipital, supraoccipital and prootic, otooccipital and basioccipital; b) complete fusion between exoccipital and opisthotic to form the otooccipital, an event which is generally observed in Squamata neonates (Maisano, 2001). For the appendicular skeleton, the considered events were: a) the presence of secondary ossification centers in all the epiphyses; b) the presence of ossification centers in the carpus; c) the fusion of astragalus and calcaneum but the suture is still discernible.

RESULTS

Description of the ossification pattern of the skeleton

The descriptions are organized as follows: skull, vertebral column, pectoral girdle and sternum complex, forelimb, pelvic girdle, and hindlimb.

Skull in *A. bogotensis*: In neonates, all dermatocranium elements are fully ossified except for frontal and parietal, since just the lateral margins are present, forming the frontoparietal

fontanelle (Fig. 2A). Ventrally, the chondrocranium is ossified, and the sphenoid, prootic, opisthotic, and exoccipital are present, but they are separated by chondral sutures; except for the basioccipital and sphenoid which have not been completely ossified and the basicranial fenestra is present between them (Fig. 3A).

In the juvenile stage, the size of the frontoparietal fontanelle and basicranial fenestra is reduced (Fig. 2B, 3B). By 36.55 mm SVL, the frontal begins to develop the frontoparietal tabs (Fig. 2B, C); in the basicranium, the exoccipital with ophistotic and supraoccipital with exoccipital are fusing (Fig. 3B, C).

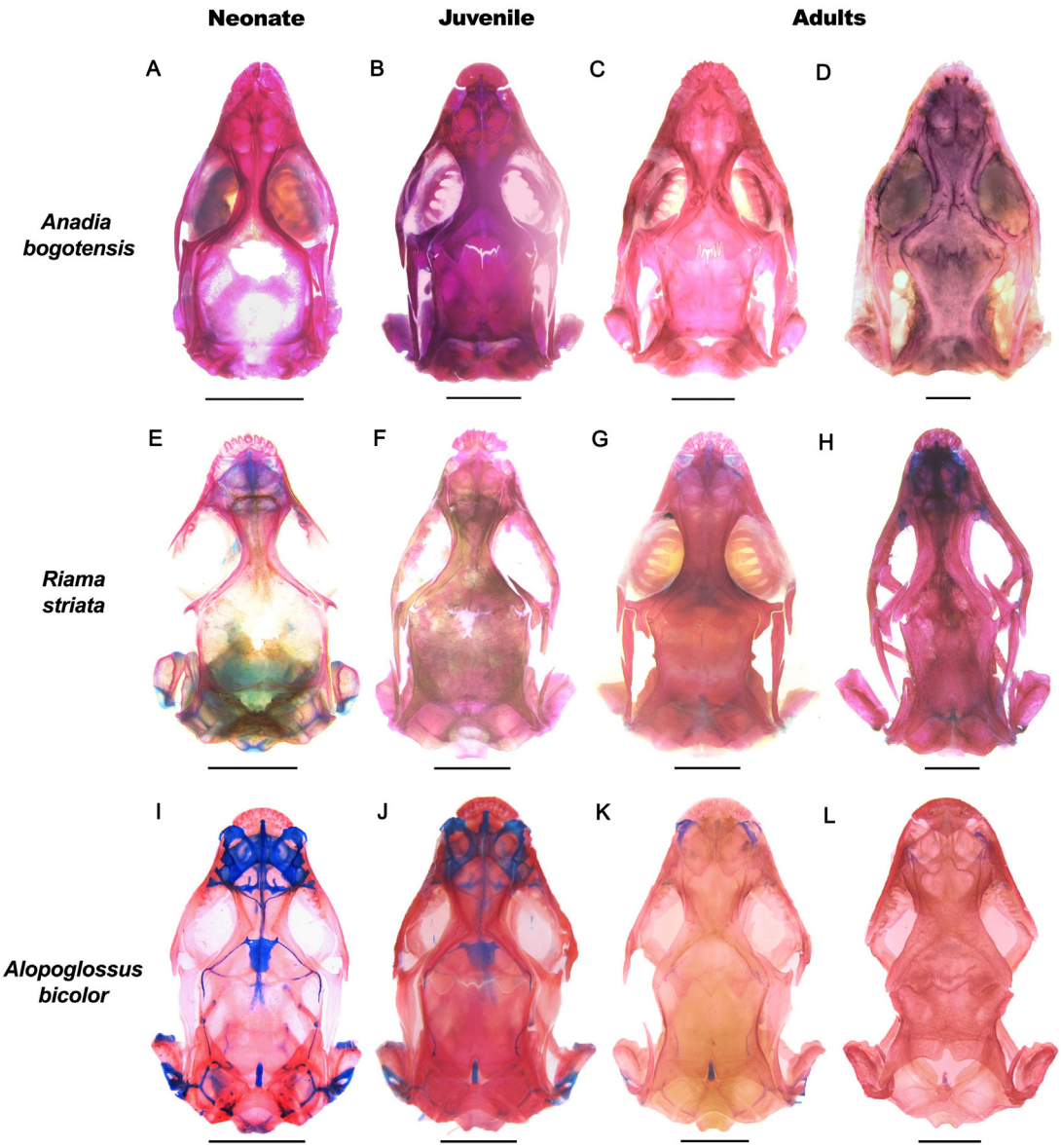

Figura 2. Secuencia de osificación postnatal del cráneo en vista dorsal, en tres especies de Gymnophthalmoidea. *Anadia bogotensis*: neonato (A, 22.86 mm SVL); juvenil (B, 36.55 mm SVL); y adultos (C, 50.0 mm SVL; D, 62.67 mm SVL). *Riama striata*: neonato (E, 28 mm SVL); juvenil (F, 38.7 mm SVL); y adultos (G, 52.63 mm SVL; H, 66.20 mm SVL). *Alopoglossus bicolor*: neonato (I, 23.8 mm SVL); juvenil (J, 44.28 mm SVL); y adultos (K, 50.24 mm SVL; L, 60.28 mm SVL). Barra de escala: 2 mm.

Figure 2. Sequence of postnatal ossification of dorsal skull in three species of Gymnophthalmoidea. *Anadia bogotensis*: neonate (A, 22.86 mm SVL); juvenile (B, 36.55 mm SVL); and adults (C, 50.0 mm SVL; D, 62.67 mm SVL). *Riama striata:* neonate (E, 28 mm SVL); juvenile (F, 38.7 mm SVL); and adults (G, 52.63 mm SVL; H, 66.20 mm SVL). *Alopoglossus bicolor*: neonate (I, 23.8 mm SVL); juvenile (J, 44.28 mm SVL); and adults (K, 50.24 mm SVL; L, 60.28 mm SVL). Scale bar: 2 mm.

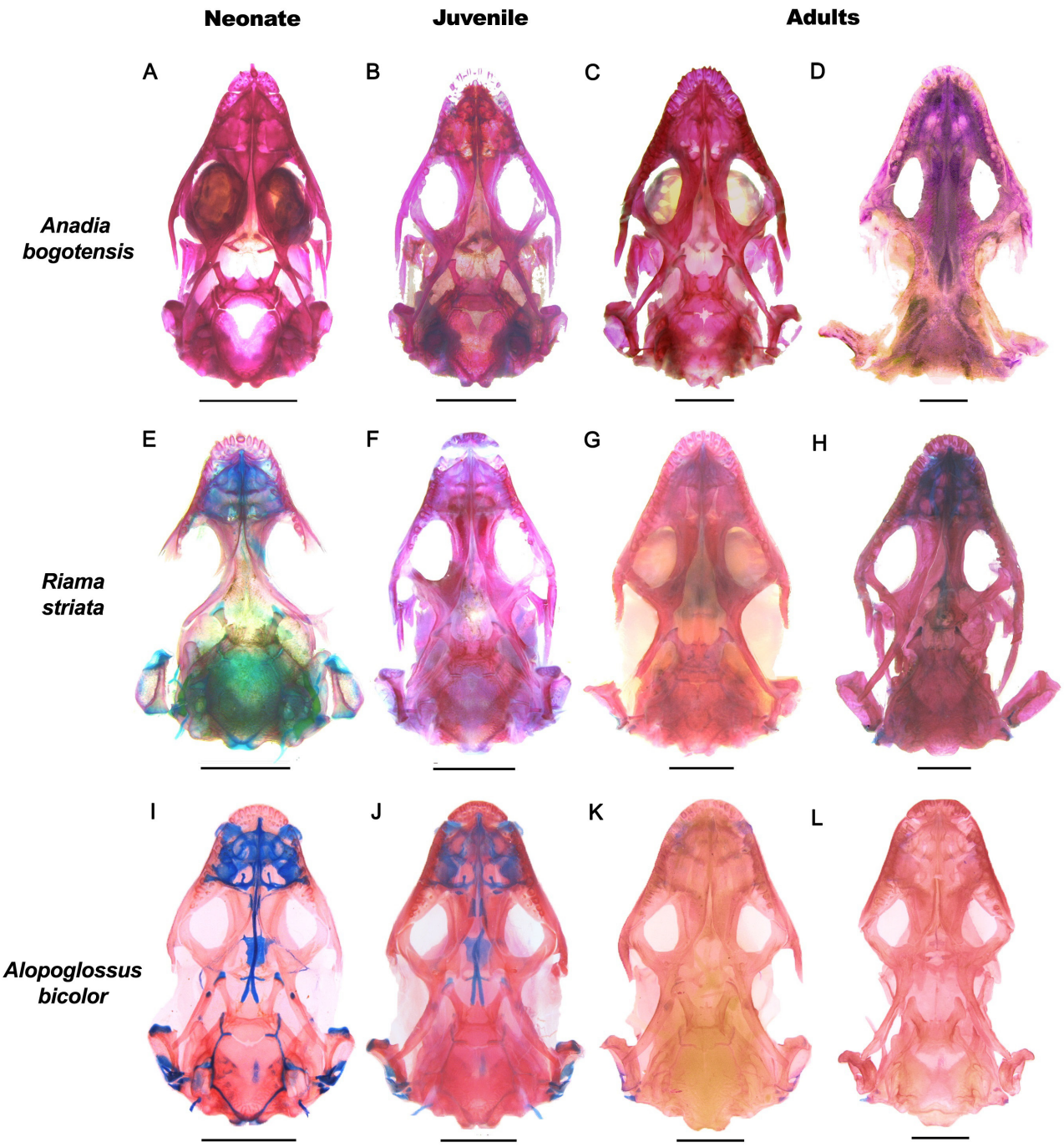

Figura 3. Secuencia de osificación postnatal del cráneo en vista ventral en tres especies de Gymnophthalmoidea. *Anadia bogotensis*: neonato (A, 22.86 mm SVL); juvenil (B, 36.55 mm SVL); y adultos (C, 50.0 mm SVL; D, 62.67 mm SVL). *Riama striata*: neonato (E, 28 mm SVL); juvenil (F, 38.7 mm SVL); y adultos (G, 52.63 mm SVL; H, 66.20 mm SVL). *Alopoglossus bicolor*: neonato (I, 23.8 mm SVL); juvenil (J, 44.28 mm SVL); y adultos (K, 50.24 mm SVL; L, 60.28 mm SVL). Barra de escala: 2 mm.

Figure 3. Sequence of postnatal ossification of ventral skull in three species of Gymnophthalmoidea. *Anadia bogotensis*: neonate (A, 22.86 mm SVL); juvenile (B, 36.55 mm SVL); and adults (C, 50.0 mm SVL; D, 62.67 mm SVL). *Riama striata*: neonate (E, 28 mm SVL); juvenile (F, 38.7 mm SVL); and adults (G, 52.63 mm SVL; H, 66.20 mm SVL). *Alopoglossus bicolor*: neonate (I, 23.8 mm SVL); juvenile (J, 44.28 mm SVL); and adults (K, 50.24 mm SVL; L, 60.28 mm SVL). Scale bar: 2 mm.

In adult stage, by 42.53 mm SVL, the opisthotic and exoccipital fuse completely to form the otooccipital, and these are fusing with the basioccipital and the prootic. By 48.63 mm SVL, the frontal and parietal are completely differentiated, the frontoparietal fontanelle is closed, the frontoparietal suture is present, and the frontoparietal tabs are well-developed (Fig. 2D). By 50 mm SVL, the otooccipital and basioccipital are fused, while the sphenoid and prootic are fusing. The basicranial fenestra is notably reduced by 50.36 mm SVL and completely closed by 52.60 mm SVL, in which all the elements of the basicranium are fused forming the otico-occipital complex (Fig. 3D).

Skull in *R. striata*: The neonates exhibit all dermatocranium elements ossified with the frontoparietal fontanelle present; the frontal and parietal ossification is complete by 66.20 mm SVL, and the fontanelle is closed (Fig. 2E-H). All elements of the basicranium are ossified, but the basicranial fenestra is open until adult stage, and it closes when it reaches 66.20 mm SVL (Fig. 3E-H). In the juvenile stage (38.7 mm SVL), supraoccipital, exoccipital, opisthotic, and basioccipital are fusing. The prootic, opisthotic, and sphenoid are fusing by 52.63 mm SVL in the adult stage. The fusion of the exoccipital with the opisthotic forming the otoccipital is observed by 52.63 mm SVL. Fusion of otooccipital, supraoccipital and basioccipital, and prootic and sphenoid occurs by 58.02 mm SVL. By 66.20 mm SVL, the fusion of the prootic with the otooccipital is observed.

Skull in *A. bicolor*: Dermatocranium is ossified in neonates, the frontoparietal fontanelle is open, and its closure occurs in adults by 51.46 mm SVL (Fig. 2I-L). The basicranium shows ossified elements; the basicranial fenestra is open, but it closes in the adult by 56.24 mm SVL (Fig. 3I-L). In the adult stage, the exoccipital and opisthotic are fusing by 44.28 mm SVL, and they are fused by 50.24 mm SVL forming the otoccipital; the otooccipital and basioccipital, and the prootic and sphenoid are fusing by 50. 24 mm SVL; and the supraoccipital, otooccipital, and prootic by 51.46 mm SVL. Finally, the complete fusion of these elements is observed in the adult of 51.92 mm SVL.

Vertebral column in *A. bogotensis*: Neonates exhibit ossified vertebral centra, but neural arches are cartilaginous. Cervical ribs and dorsal ribs are ossified with cartilaginous distal ends; while sternal ribs exhibit the vertebrocostal segment ossified, and the intercostal segment ossifying. In the juvenile stage, the neural arches begin to ossify. Finally, the neural arches are completely ossified in the adult of 42.53 mm SVL and all ribs by 48.63 mm SVL.

Vertebral column in *R. striata* and *A. bicolor*: The neural arches are completely ossified in adults of 58.02 mm SVL in *R. striata* and 54.4 mm SVL in *A. bicolor*. The complete ossification of the ribs is observed in the adult of 52.63 mm SVL in *R. striata* and 54.4 mm SVL in *A. bicolor*.

Pectoral girdle in *A. bogotensis*: The unpaired element of dermal origin, clavicle, and interclavicle are well differentiated in neonates. The chondral elements like coracoid and scapula are completely ossified, but the epicoracoid and suprascapula are cartilaginous, while the pre-sternum and meso-sternum begin to calcify. At the juvenile stage, calcification increases in the epicoracoid, pre-sternum and meso-sternum, which at 50 mm in the adult stage are completely calcified, and the coracoid and scapula are fused.

Pectoral-sternum girdle complex in *R. striata* and *A. bicolor*: The complete calcification of the pre-sternum and meso-sternum, and the fusion of the scapula and coracoid occurs in adults at 52.63 mm SVL in *R. striata*, and 51.92 mm SVL in *A. bicolor*.

Forelimb in *A. bogotensis*: In the neonatal stage, all diaphyses are well ossified and SCs are present in the humeral, ulnar, distal metacarpal, and proximal phalangeal epiphyseal cartilages (Fig. 4a). Additionally, OCs are observed in carpal elements, except for distal carpal 1 (Fig. 4A). The pisiform and the palmar sesamoids are cartilaginous nodules, but the distal phalangeal sesamoids are ossifying (Table 1).

At juvenile stage, a SC is present in proximal metacarpal epiphyseal cartilages and an OC in distal carpal 1 by 36.55 mm SVL (Fig. 4B). The cartilaginous sesamoid located between proximal radial and ulnar epiphysis is observed and the ulnar patella is ossifying (Table 1). At this stage, the apophyseal ossifications begin to develop (Table 2).

In adults, by 42.53 mm SVL all carpals are completely ossified (Fig. 4C-D). Sutures are present between ossified epiphyses and diaphyses of the humerus, radius, ulna, and proximal metacarpals by 48.63 mm SVL, while in the distal metacarpals the suture is present at 50 mm SVL and in the proximal phalanges by 50.36 mm SVL. In the adult of 52.60 mm SVL, the proximal humeral epiphysis fuses completely to the diaphysis. No changes were recorded in larger individuals analyzed, and there is no complete fusion of epiphyses of the zeugopodium (radius, ulna) and autopodium (metacarpals, phalanges).

Other sesamoids continue to develop in adults, and they ossify

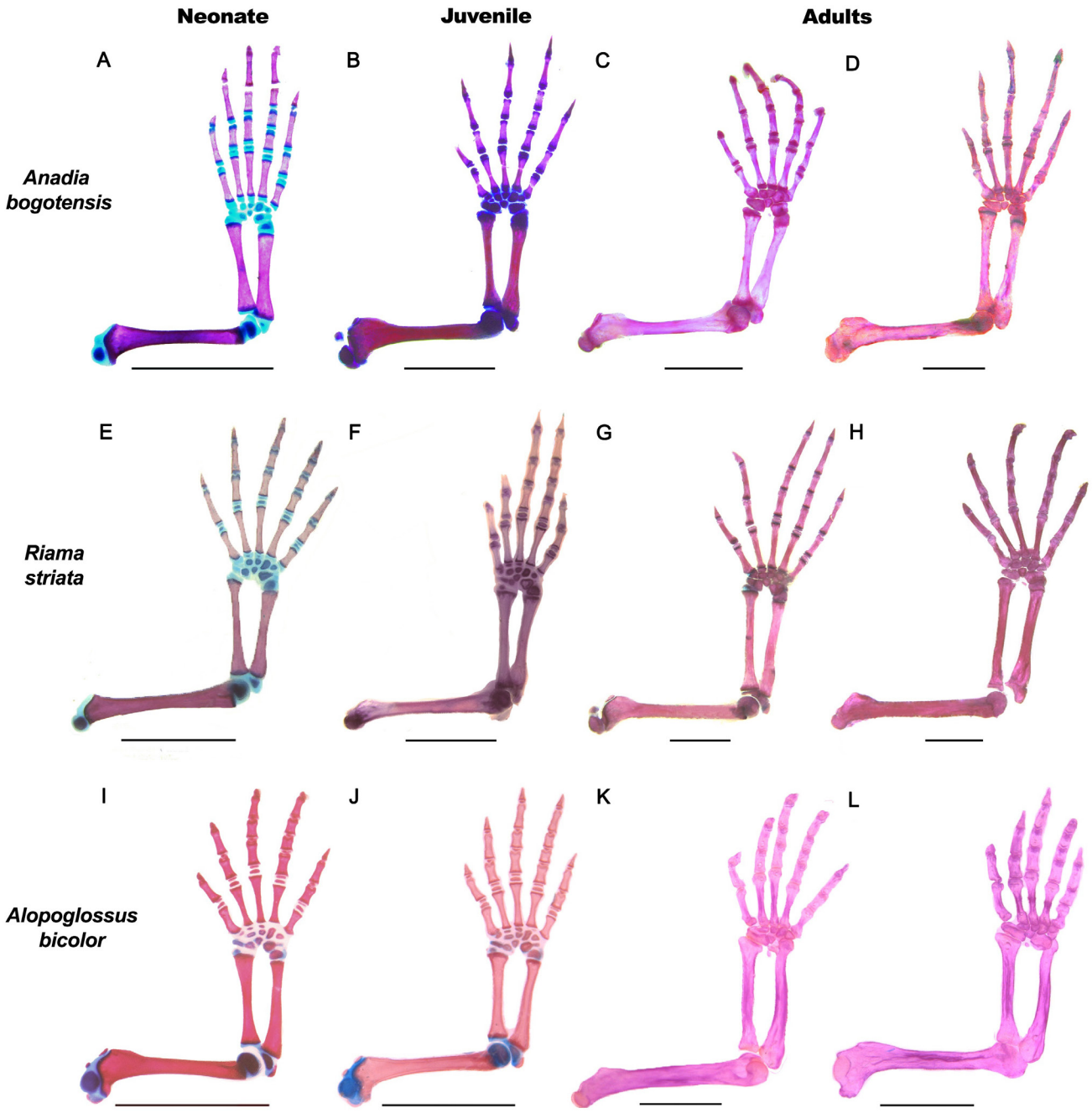

Figura 4. Secuencia de osificación postnatal de la extremidad anterior en tres especies de Gymnophthalmoidea. *Anadia bogotensis*: neonato (A, 22.23 mm SVL); juvenil (B, 36.55 mm SVL); y adultos (C, 50.36 mm SVL; D, 62.67 mm SVL). *Riama striata*: neonato (E, 28.85 mm SVL); juvenil (F, 38.7 mm SVL); y adultos (G, 52.63 mm SVL; H, 66.20 mm SVL). *Alopoglossus bicolor*: neonato (I, 20.22 mm SVL); juvenil (J, 30.24 mm SVL); y adultos (K, 51.92 mm SVL; L, 54.4 mm SVL). Barra de escala: 2 mm.

Figure 4. Sequence of postnatal ossification of forelimb in three species of Gymnophthalmoidea. *Anadia bogotensis*: neonate (A, 22.23 mm SVL); juvenile (B, 36.55 mm SVL); and adults (C, 50.36 mm SVL; D, 62.67 mm SVL). *Riama striata*: neonate (E, 28.85 mm SVL); juvenile (F, 38.7 mm SVL); and adults (G, 52.63 mm SVL; H, 66.20 mm SVL). *Alopoglossus bicolor*: neonate (I, 20.22 mm SVL); juvenile (J, 30.24 mm SVL); and adults (K, 51.92 mm SVL; L, 54.4 mm SVL). Scale bar: 2 mm.

Tabla 1. Distribución de los sesamoides en *Anadia bogotensis*, *Riama striata* and *Alopoglossus bicolor* durante la ontogenia, en los estados neonato (N), juvenil (J) y adulto (A) y en diferentes tamaños (SVL, mm, excepto en el neonato de *A. bicolor* que corresponde a BL).

Table 1. Distribution of the sesamoids in *Anadia bogotensis*, *Riama striata* and *Alopoglossus bicolor* during ontogeny, including neonate (N), juvenile (J) and adult (A) stages, and specimen size (SVL, mm, except in the neonate of *A. bicolor*, which corresponds to BL).

Sesamoids	*A. bogotensis*					*R. striata*				*A. bicolor*		
	N	J		A		N	J	A		N	J	A
	26.46	36.55	42.53	48.63	50	28	38.7	52.63	58	20.2	30.24	51.92
Pisiform	x	x	x	x	x	x	x	x	x	x	x	x
Distal phalangeal sesamoids in manus and pes	x	x	x	x	x	x	x	x	x	x	x	x
Tibial lunula	x	x	x	x	x	x	x	x	x	x	x	x
Palmar sesamoid	x	x	x	x	x	x	x	x	x	x	x	x
Plantar sesamoid	x	x	x	x	x	x	x	x	x	x	x	x
Ulnar patella	x	x	x	x	x	x	x	x	x	x	x	x
Post-axial ligament sesamoid (fabella)	x	x	x	x	x	x	x	x	x	x	x	x
Tibial patella	x	x	x	x	x	x	x	x	x	x	x	x
Parafibula		x	x	x	x		x	x	x		x	x
Dorsal pre-axial tibio femoral lunula			x	x	x		x	x	x		x	x
Ventral pre-axial tarsal sesamoid				x	x		x	x	x		x	x
Dorsal pre-axial tibio femoral lunula			x	x	x							
Sesamoid ventral to the distal femoral epiphysis		x	x	x	x							
Sesamoid dorsal to the proximal radial epiphysis		x	x	x	x							
Sesamoid dorsal located between distal tarsal IV and metatarsal IV		x	x	x	x							
Sesamoid ventral to the proximal radial epiphysis			x	x	x							
Sesamoid dorsal to the articulation of radiale with metacarpal I				x	x							
Sesamoid between distal ulnar and radial epiphyses					x							x
Sesamoid anterior to the pisiform					x				x			
Sesamoid ventral to the articulation of the proximal tarsal and metatarsal I									x			
Ventral pre-axial tibio femoral lunula									x			
Sesamoid dorsal to the proximal radial epiphysis									x			

Tabla 1 (cont.). Distribución de los sesamoides en *Anadia bogotensis, Riama striata* and *Alopoglossus bicolor* durante la ontogenia, en los estados neonato (N), juvenil (J) y adulto (A) y en diferentes tamaños (SVL, mm, excepto en el neonato de *A. bicolor* que corresponde a BL).

Table 1 (cont.). Distribution of the sesamoids in *Anadia bogotensis, Riama striata* and *Alopoglossus bicolor* during ontogeny, including neonate (N), juvenile (J) and adult (A) stages, and specimen size (SVL, mm, except in the neonate of *A. bicolor*, which corresponds to BL).

Sesamoids	*A. bogotensis*					*R. striata*				*A. bicolor*		
	N	J		A		N	J		A	N	J	A
	26.46	36.55	42.53	48.63	50	28	38.7	52.63	58	20.2	30.24	51.92
Sesamoid lateral and distal to the distal epiphysis of metatarsal V												x
Sesamoid located between proximal radial and ulnar epiphysis												x
Sesamoid dorsal to the articulation of ulnare with metacarpal IV												x
Ventral ligament sesamoid (in the ligaments ventral to the knee)												x

by 50 mm SVL (Table 1). Apophyseal ossifications are observed in the adult of 42.53 mm SVL, but in individuals of 50 mm SVL they are completely fused (Table 2).

Forelimb in *R. striata*: The 28.85 mm SVL neonate presents SCs in the humeral, ulnar, metacarpals II and III and proximal phalangeal epiphyseal cartilages, and OCs in the carpal elements, except the distal carpal 1 (Fig. 4E). In the 38.7 mm SVL juvenile, SCs appear on distal radial and proximal metacarpal I epiphyseal cartilages (Fig. 4F). In adult stage, by 52.63 mm SVL, the SC of the proximal radial epiphyseal cartilage and the OC in distal carpal 1 are present, and the proximal humeral, metacarpals, and phalangeal epiphyseal cartilages are completely ossified with epiphyseal sutures (Fig. 4G). By 58.02 mm SVL, epiphyseal suture in radius, ulna, and distal humerus are visible, and the fusion is complete in the proximal epiphysis of the humerus and metacarpals I, II, III. By 66.2 mm SVL, fusion of the distal epiphysis of the ulna and all the epiphyses of the metacarpals is complete. Some epiphyses do not completely fuse in the zeugopodium (radius and ulnar proximal epiphysis) and autopodium (phalanges, Fig. 4H). *R. striata* develops six sesamoids from neonate to adult (Table 1); the apophyseal ossifications are observed between the juvenile of 38.7 mm SVL and the adult of 52.63 mm SVL (Table 2).

Forelimb in *A. bicolor*: Neonate (20.2 mm BL) exhibits SCs in all the epiphyses of the limb, except for the proximal radius and the proximal metacarpals V (Fig. 4I). Distal carpal 1 is the only one that does not exhibit an OC in the carpus. In adult stage, epiphyseal sutures are present in the humerus, radius, ulna, distal metacarpal, and proximal phalangeal by 50.24 mm SVL but also, in this same specimen, the fusion of the proximal metacarpals epiphyses and complete carpal ossification are evident. Subsequently, by 51.92 mm SVL the epiphyses and diaphyses of the forelimb are completely fused except the radius, which is completed by 54.4 mm SVL in the distal epiphyses and by 56.24 mm SVL in the proximal ones (Fig. 4K, L). *A. bicolor* exhibits sesamoids that develop between the neonate and the adult (Table 1). Apophyseal ossifications occur in the juvenile by 30.24 mm SVL and the adult by 50.24 mm SVL (Table 2), which fuse completely above this size.

Pelvic girdle *A. bogotensis*: Neonate (26.46 mm SVL) presents the ischium and pubis fully ossified but not fused. Ischiatic symphysis presents endochondral ossification, while epipubis, ischiatic process, and the distal tip of the ilium are chondral, and the ossification begins in juveniles. In adults, the fusion between pubis, ischium, and ilium is observed by 58.23 mm SVL.

Pelvic girdle in *R. striata* and *A. bicolor*: In *R. striata*, pubis, ischium, and ilium are completely fused at 58.02 mm SVL. In *A. bicolor* the epipubis and ischial symphysis begin to ossify in the neonate by 20.2 mm BL, and pelvic bones are fused by 50.24 mm SVL.

Tabla 2. Osificaciones apofisiárias en *Anadia bogotensis*, *Riama striata* y *Alopoglossus bicolor* durante la ontogenia, en los estados neonato (N), juvenil (J) y adulto (A) en diferentes tamaños (SVL, mm).

Table 2. Apophyseal ossifications in *Anadia bogotensis*, *Riama striata* and *Alopoglossus bicolor* during ontogeny, including neonate (N), juvenile (J) and adult (A) stages, and specimen size (SVL, mm)..

Apophyseal ossifications	*A. bogotensis*		*R. striata*		*A. bicolor*	
	J	A	J	A	J	A
	36.55	42.5	38.7	52.63	30.24	50.24
On the preaxial edge of the proximal humeral epiphyseal cartilage	x	x	x	x	x	
On the postaxial edge of the proximal humeral epiphyseal cartilage	x	x	x	x	x	
On the preaxial edge of the distal ulnar epiphyseal cartilage	x	x	x		x	
On the postaxial edge of the distal ulnar epiphyseal cartilage	x	x				
On the postaxial edge of the distal metacarpal V epiphyseal cartilage	x	x				x
On the preaxial edge of the distal femoral epiphyseal cartilage	x	x		x		x
On the postaxial edge of the proximal fibular epiphyseal cartilage	x	x				
On the postaxial edge of the distal fibular epiphyseal cartilage	x	x				
On the postaxial edge of the proximal metacarpal V epiphyseal cartilage	x	x				
On the dorsal central aspect of the proximal humeral epiphyseal cartilage		x	x		x	
On the dorsal aspect near to preaxial edge of the distal humeral epiphyseal cartilage		x	x	x	x	
On the dorsal aspect near to postaxial edge of the distal humeral epiphyseal cartilage		x	x	x	x	
On the preaxial edge of the distal radial epiphyseal cartilage		x			x	x
On the postaxial edge of the proximal metacarpal IV epiphyseal cartilage		x				
On the postaxial edge of the distal femoral epiphyseal cartilage		x	x	x		x
On the preaxial edge of the proximal fibular epiphyseal cartilage		x			x	
On the preaxial edge of the distal tibial epiphyseal cartilage		x			x	
On the postaxial edge of the proximal ulnar epiphyseal cartilage					x	
On the preaxial edge of the proximal radial epiphyseal cartilage			x			
On the postaxial edge of the distal metacarpal I epiphyseal cartilage			x			
On the ventral aspect of the radiale					x	
On the postaxial edge of the proximal femoral epiphyseal cartilage				x	x	
On the preaxial edge of the proximal femoral epiphyseal cartilage				x	x	

Hindlimb in *A. bogotensis*: In neonates, the diaphyses are ossified, and the femoral, distal metatarsal, and phalangeal epiphyseal cartilages exhibit SCs (Fig. 5A). Likewise, the astragalus, calcaneum and distal tarsal 3 and 4 present OCs (Fig. 5A). There are three sesamoids, plantar sesamoids (26.5 mm SVL) and tibial lunula (22.8 mm SVL) present as cartilaginous nodules, and the distal phalangeal sesamoids (22.8 mm SVL) are in the process of ossification (Table 1).

The juvenile, by 36.55 mm SVL, exhibits SCs in the distal fibular and proximal metatarsal epiphyseal cartilages (Fig. 5B). The proximal tibial epiphysis is fully ossified, and the suture with the diaphysis is observed; in the tarsus, the astragalus and calcaneum are ossified with a suture between them. Other sesamoids are present in ossification (Table 1), and apophyseal ossifications begin to be observed (Table 2).

In the adult stage, by 42.53 mm SVL, the proximal fibular and distal tibial epiphyseal cartilages exhibit SCs. By 48.63 mm SVL, the proximal femoral, distal tibial, and metatarsals epiphyses are fusing with the diaphyses, and fusion of the astragalus and calcaneum is complete. While the fibular, the distal femoral, the metatarsals, and the proximal phalangeal epiphyses are fusing by 50 mm SVL, the distal tarsals 3 and 4 are completely ossified

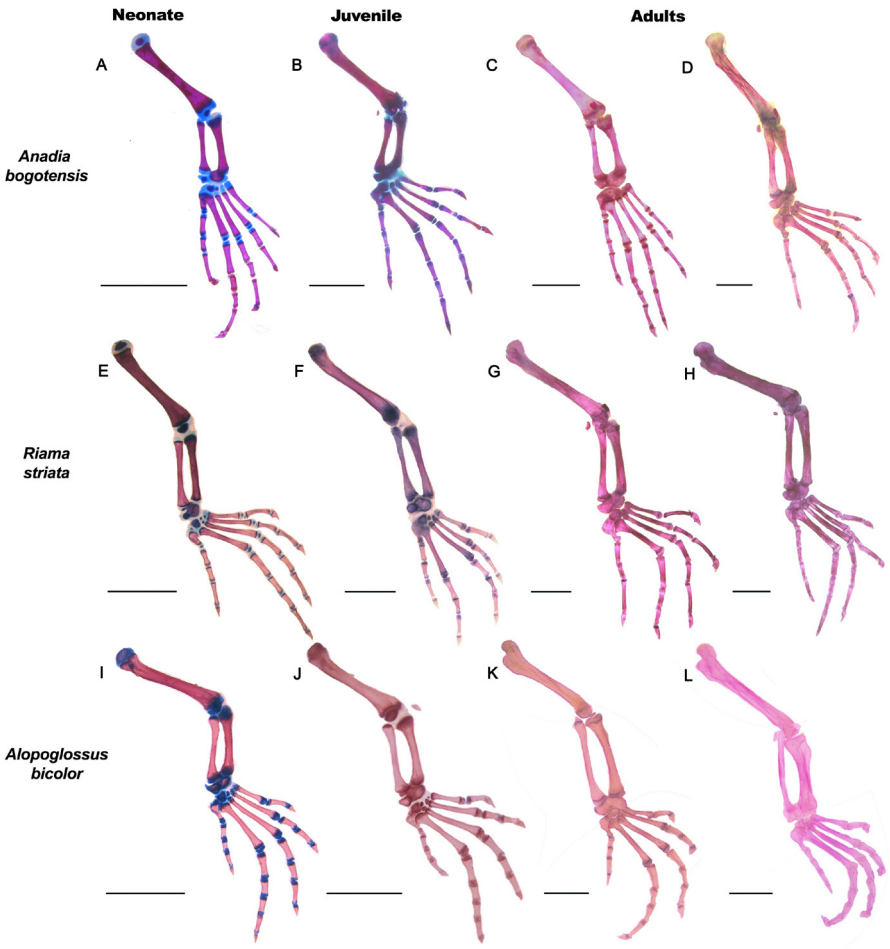

Figura 5. Secuencia de osificación postnatal de la extremidad posterior en tres especies de Gymnophthalmoidea. *Anadia bogotensis*: neonato (A, 22.23 mm SVL); juvenil (B, 36.55 mm SVL); y adultos (C, 50.36 mm SVL; D, 62.67 mm SVL). *Riama striata*: neonato (E, 28.85 mm SVL); juvenil (F, 38.7 mm SVL); y adultos (G, 58.02 mm SVL; H, 66.20 mm SVL). *Alopoglossus bicolor*: neonato (I, 20.22 mm BL); juvenil (J, 30.24 mm SVL); y adultos (K, 50.24 mm SVL; L, 55.12 mm SVL). Barra de escala: 2 mm.

Figure 5. Sequence of postnatal ossification of hindlimb in three species of Gymnophthalmoidea. *Anadia bogotensis*: neonate (A, 22.23 mm SVL); juvenile (B, 36.55 mm SVL); and adults (C, 50.36 mm SVL; D, 62.67 mm SVL). *Riama striata:* neonate (E, 28.85 mm SVL); juvenile (F, 38.7 mm SVL); and adults (G, 58.02 mm SVL; H, 66.20 mm SVL). *Alopoglossus bicolor*: neonate (I, 20.22 mm BL); juvenile (J, 30.24 mm SVL); and adults (K, 50.24 mm SVL; L, 55.12 mm SVL). Scale bar: 2 mm.

(Fig. 5C). By 58.23 mm SVL, the proximal femoral, metatarsals, and phalangeal I-II epiphyses are fused with diaphyses. The rest of the elements remain with suture, even in the largest individual analyzed at 62.67 mm SVL (Fig. 5D). Other ossified sesamoids develop in adults between 42.5 mm to 50 mm SVL (Table 1). The apophyseal ossifications are observed in the adult of 42.53 mm SVL, and they are fused by 50.36 mm SVL (Table 2).

Hindlimb in *R. striata*: In the neonate, the SCs are present in the distal fibular, metatarsal, and proximal phalangeal epiphyseal cartilages by 28 mm SVL (Fig. 5E); in this stage, all tarsal elements present OCs. The juvenile (38.7 mm SVL) exhibit SCs in the distal tibial and the proximal metatarsal I epiphyseal cartilages (Fig. 5F). In the adult of 52.63 mm SVL, the proximal tibial and fibular epiphyseal cartilages present SCs, and the proximal tarsal elements are fused with a suture between them. By 58.02 mm SVL, the complete ossification with suture is observed in the distal femoral, tibial, fibular, metatarsal, and proximal phalangeal epiphyses (Fig. 5G). The complete fusion of the proximal femoral and metatarsals epiphyses, and astragalus with calcaneum is observed by 58.02 mm SVL. By 66.20 mm SVL, complete fusion of phalangeal proximal epiphyses is evident (Fig. 5H). The sesamoids are observed from the neonate and continuing their development during ontogeny (Table 1). Apophyseal ossifications were observed between juveniles by 38.7 mm SVL and adults by 52.63 mm SVL (Table 2).

Hindlimb in *A. bicolor*: Neonate by 20.22 mm SVL presents SCs in all epiphyseal cartilages except in the proximal fibula, distal tibia, and proximal metatarsals I, II, IV (Fig. 5I). At the adult stage, 50.24 mm SVL, the complete ossification, and suture are observed in the epiphyses of the femur, tibia, fibula, metatarsals, and proximal phalanges. Ossification of the tarsal elements and complete fusion of the astragalus and calcaneum are also noticed (Fig. 5K). By 51.92 mm SVL, the fusion is complete in metatarsal, proximal femur, and phalangeal epiphyses, while the fusion in the other epiphyses occurs by 54.4 mm SVL (Fig. 5l). The development of sesamoids is observed from neonates to adults (Table 1). The apophyseal ossifications are observed between 30.24 mm SVL and 50.24 mm SVL and, after this size, they fuse and are no longer observed (Table 2).

Ossification sequences and rank analysis

Ossification sequences of skull and limbs were established in four species as shown in Table 3. In total, 88 events were analyzed in total: 21 for skull, 35 for forelimb, and 32 for hindlimb. The variation in the ranges of all skeletal elements of the four analyzed species is shown in figure 6.

For the dermatocranium, the development of the cranial roof involves the complete differentiation of the frontal and parietal with the closure of the frontoparietal fontanelle. This occurs in small to medium-sized adults of the analyzed species after sexual maturity is reached (Fig. 6, Fr-co, P-co). For the chondrocranium, the onset of fusion of bony elements, when the suture is present, occurs in juveniles (Fig. 6, Ot Fs, So+Eo Fs, Ot+Bo Fs, Pro+Ot Fs, Pro+Bs Fs). Finally, the complete fusion of the basicranium elements to form the otico-occipital complex occurs in large adult specimens, late into ontogeny (Fig. 6, So+Eo Fc, Pro+Ot Fc, Pro+Bs Fc, Bo+Bs Fc).

In the limbs, all species present ossified diaphyses and the significant events are related to the ossification of epiphyseal cartilages and basipodial elements. These species share events at the beginning of post-embryonic development since neonates exhibit SCs in epiphyseal cartilages (Fig. 6, p H Sc, d H Sc, p Ul Sc, d Ul Sc, d Mc Sc, p Fp Sc, p Mc Sc, p Hp Sc, p Mt Sc, d Fi Sc, p FS c) and OCs in the carpus, with the exception of distal carpal 1 (Fig. 6, r, u, i).

In the juvenile stage, the analyzed species shared these events: other epiphyseal cartilages develop SCs (Fig. 6, d Ra Sc, p Fi Sc, d Ti Sc, p Ra Sc); the ossification of distal carpal 1 (Fig. 6, Cd 1); the fusion with suture of calcaneus and astragalus (Fig. 6, Ast + Cal Fs); and the complete ossification of epiphyses, with a suture with the diaphyses (Fig. 6, p Mt Fs, p Fp Fs, d Mc Fs, p Ti Fs, p Ti Fs, p F Fs, d Ra Fs, d Ul Fs, p H Fs, d Ti Fs, p Mc Fs, p Ti Fs, p F Fs, d Fi Fs, d Fi Fs, d Mt Fs, p Hp Fs, d H Fs, p Ul Fs, p Ra Fs, d F Fs).

Finally, the complete fusion of epiphyses with diaphyses is observed at the end of juvenile stage and during the adult stage (Fig. 6, p Mt Fc, p Fp Fc, p Mc Fc, d H Fc, p Ul Fc, d F Fc, p Fi Fc, p Ti Fc, d Ti Fc, d Fi Fc, d Mc Fc, p H Fc, d Ra Fc, p F Fc, p Mt Fc, d Ul Fc, p Hp Fc, p Ra Fc).

Heterochronies

Based on PGi-Parsimov analysis carried out in neonatal specimens, Gymnophthalmidae shares an ossification heterochronic events in which the development of SCs in radial epiphyseal cartilages occurs later than in the humeral, ulnar, metacarpal, and femoral epiphyseal cartilages, and OCs in the carpus (Fig. 7).

On the other hand, each species is characterized by a heterochronic event that constitutes autapomorphies (Fig. 7). As a result, for *A. bogotensis*, the development of SCs in the fibular epiphyseal cartilages occurs later than humeral, ulnar, metacarpal, femoral, and metatarsal epiphyseal cartilages,

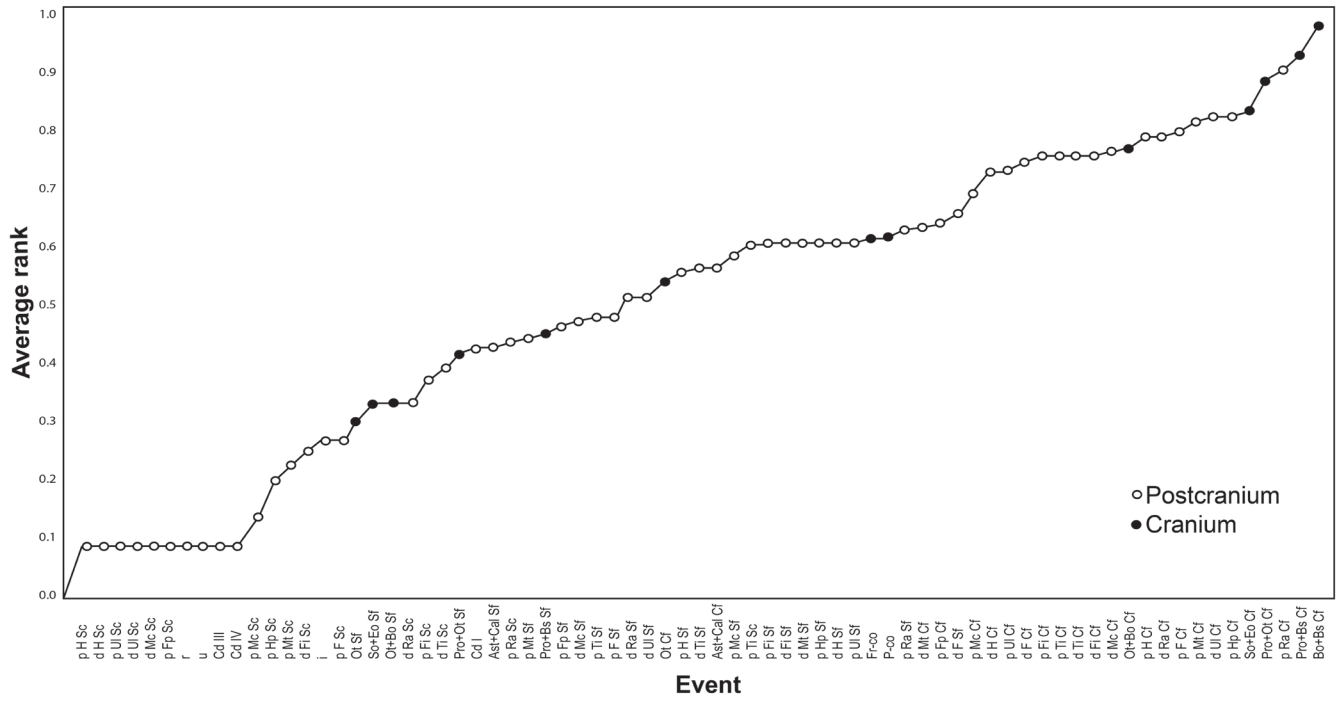

Figura 6. Análisis de rangos de los eventos de osificación de *A. bogotensis, R. striata, A. bicolor* y *B. bicolor*. Neonatos en el extremo izquierdo de la gráfica y adultos en el extremo derecho. Abreviaciones para los eventos: Cf, fusión completa; Sc, centro secundario de osificación; Sf, fusionando con sutura presente. Abreviaciones para el cráneo: Bo, basioccipital; Bs, esfenoides; Eo, exoccipital; Fr-co, osificación completa del frontal; Fr-io, osificación incompleta del frontal; P-co, osificación completa del parietal; P-io, osificación incompleta del parietal; Pro, proótico; Ot, otoccipital; So, supraoccipital. Abreviaciones para extremidades: Ast+Cal, astrágalo y calcáneo; Cd I, II, III, IV, V, carpales distales 1-5; d, epífisis distal; H, húmero; Hp, falanges extremidades posteriores; F, fémur; Fi, fíbula; Fp, falanges extremidades anteriores; i, central; Mc, metacarpales; Mt, metatarsales; p, epífisis proximal; r, radial; Ra, radio; u, ulnar; Ul, ulna; Td III, IV, tarsales distales 3 y 4; Ti, tibia. Los eventos sin p o d incluyen los dos extremos del hueso.

Figure 6. Ranks analysis for ossification events standardized of *A. bogotensis, R. striata, A. bicolor* and *B. bicolor*. On the left neonates, on the right adults. Abbreviations for events: Cf, complete fusion of elements; Sc, secondary center of ossification; Sf, fusing and suture present. Abbreviations for skull elements: Bo, basioccipital; Bs sphenoid; Eo, exoccipital; Fr-co, frontal complete ossification; Fr-io, frontal incomplete ossification; P-co, parietal complete ossification; P-io, parietal incomplete ossification; Pro, prootic; Ot, otoccipital; So, supraoccipital. Abbreviations for limbs elements: Ast+Cal, astragalus and calcaneum; Cd I, II, III, IV, V, distal carpals 1-5; d, distal epiphyseal cartilages; H, humerus; Hp, hindlimb phalangeal cartilages; F, femur; Fi, fíbula; Fp, forelimb phalanges; i, centrale; Mc, metacarpals, Mt, metatarsals; p, proximal epiphyseal cartilages; r, radiale; Ra, radius; u, ulnare; Ul, ulna; Td 3, 4, distal tarsals III and IV; Ti, tibia. The postcranial events without p or d refers both.

and OCs in the carpal elements. In *R. striata*, the fusion with suture between astragalus and calcaneus occurs later than the fusion with suture between supraoccipital and exoccipital and the development of SCs in the tibial epiphyseal cartilage. In *B. bicolor*, the fusion between the exoccipital and opisthotic, that gives rise to the otoccipital, occurs earlier than the appearance of SCs in radial epiphyseal cartilage and the fusion with suture of the prootic with the supraoccipital and the otooccipital with the basioccipital. Finally, in *A. bicolor* the fusion with suture of the astragalus and calcaneum occurs later than the development of SCs in the radial, tibial, and fibular epiphyseal cartilages.

DISSCUSION

The analyzed species share events of the ossification pattern, but there are differences of phylogenetic importance, as well as in heterochronic events for Gymnophthalmidae (Fig. 7), and therefore, this study highlights the relevance of morphological information in comparative analyses.

Skull

In the skull, the rank analysis established that *A. bogotensis*, *R. striata*, *A. bicolor* and *B. bicolor* are similar in the development of the dermatocranium, as the frontoparietal fontanelle present

Tabla 3. Secuencia de osificación del esqueleto en *Anadia bogotensis, Riama striata, Bachia bicolor* y *Alopoglossus bicolor*. Abreviaciones para eventos: Cf, fusión completa; S, separados; Sc, centro secundario de osificación; Sf, fusionando y sutura presente. Abreviaciones para el cráneo: Bo, basioccipital; Bs, esfenoides; Eo, Exoccipital; Fr-co, osificación completa del frontal; Fr-io, osificación incompleta del frontal; P-co, osificación completa del parietal; P-io, osificación incompleta del parietal; Pro, proótico; Ot, otoccipital; So, supraoccipital. Abreviaciones para extremidades: Ast+Cal, astrágalo y calcáneo; Cd I, II, III, IV, V, carpales distales 1-5; d, epífisis distal; H, húmero; Hp, falanges extremidades posteriores; F, fémur; Fi, fíbula; Fp, falanges extremidades anteriores; i, central; Mc, metacarpales; Mt, metatarsales; p, epífisis proximal; r, radial; Ra, radio; u, ulnar; Ul, ulna; Td III, IV, tarsales distales 3 y 4; Ti, tibia. Los eventos sin p o d incluyen los dos extremos del hueso.

Table 3. Ossification sequences in the skeleton of *Anadia bogotensis, Riama striata, Bachia bicolor* and *Alopoglossus bicolor*. Abbreviations for events: Cf, complete fusion; S, separate; Sc, secondary center of ossification; Sf, fusing and suture present. Abbreviations for skull: Bo, basioccipital; Bs, sphenoid; Eo, exoccipital; Fr-co, frontal complete ossification; Fr-io, frontal incomplete ossification; P-co, parietal complete ossification; P-io, parietal incomplete ossification; Pro, prootic; Ot, otoccipital; So, supraoccipital. Abbreviations for limbs: Ast+Cal, astragalus and calcaneum; Cd I, II, III, IV, V, distal carpals 1-5; d, distal epiphyseal cartilages; H, humerus; Hp, hindlimb phalangeal cartilages; F, femur; Fi, fíbula; Fp, forelimb phalanges; i, centrale; Mc, metacarpals; Mt, metatarsals; p, proximal epiphyseal cartilages; r, radiale; Ra, radius; u, ulnare; Ul, ulna; Td III, IV, distal tarsals 3 and 4; Ti, tibia; The events without P or D refers both.

Species	Rank	Skull	Limbs
	1	Fr-io, P-io, Bo+Bs S, So+Eo S, Ot S, Ot+Bo S, Pro+Ot S, Pro+Bs S	H Sc, Ul Sc, d Mc Sc, p Fp Sc, i, r, u, cd II, III, IV y V, F Sc, d Mt Sc, p Hp Sc, Ast+Cal S, Td III y IV
	2		p Mc Sc
	3	So+Eo Sf, Ot Sf	Cd I, p Ti Sf, d Fi Sc, p Mt Sc, Ast+Cal Sf
	4	Ot Cf, Ot+Bo Sf, Pro+Ot Sf	d Ti Sc, p Fi Sc
	5	Fr-co, P-co	H Sf, Ra Sf, Ul Sf, p Mc Sf, p F Sf, d Ti Sf, p Mt Sf, Ast+Cal Cf
	6	Ot+Bo Cf, Pro+Bs Sf	d Mc Sf, d F Sf, Fi Sf, d Mt Sf, p Hp Sf
	7		p Mc Cf, p Fp Sf
	8	Bo+Bs Cf, So+ Eo Cf, Pro+Ot Cf, Pro+Bs Cf	p H Cf
	9		p F Cf, p Mt Cf
R. striata	1	Fr-io, P-io, Bo+Bs S, So+Eo S, Ot S, Ot+Bo S, Pro+Ot S, Pro+Bs S	H Sc, Ul Sc, d Mc Sc, p Fp Sc, i, r, u, Cd II, III, IV y V, F Sc, d Fi Sc, d Mt Sc, Ast+Cal S, Td III y IV
	2		p Mc Sc, p Mt Sc, p Hp Sc
	3	So+Eo Sf, Ot Sf, Ot+Bo Sf	d Ra Sc, d Ti Sc
	4	Ot Cf, Pro+Ot Sf, Pro+Bs Sf	p H Sf, p Ra Sc, Mc Sf, p Fp Sf, Cd I, p Ti Sc, p Fi Sc, Ast+Cal Sf
	5	So+Eo Cf, Ot+Bo Cf, Pro+Bs Cf	p H Cf, d H Sf, Ra Sf, Ul Sf, p Mc Cf, p F Cf, d F Sf, Ti Sf, Fi Sf, p Mt Cf, d Mt Sf, p Hp Sf, Ast+Cal Cf
	6	Fr-co, P-co, Bo+Bs Cf, Pro+Ot Cf	d Ul Cf, d Mc Cf, p Hp Cf

Tabla 3 (cont.). Secuencia de osificación del esqueleto en *Anadia bogotensis, Riama striata, Bachia bicolor* y *Alopoglossus bicolor*. Abreviaciones para eventos: Cf, fusión completa; S, separados; Sc, centro secundario de osificación; Sf, fusionando y sutura presente. Abreviaciones para el cráneo: Bo, basioccipital; Bs, esfenoides; Eo, Exoccipital; Fr-co, osificación completa del frontal; Fr-io, osificación incompleta del frontal; P-co, osificación completa del parietal; P-io, osificación incompleta del parietal; Pro, proótico; Ot, otoccipital; So, supraoccipital. Abreviaciones para extremidades: Ast+Cal, astrágalo y calcáneo; Cd I, II, III, IV, V, carpales distales 1-5; d, epífisis distal; H, húmero; Hp, falanges extremidades posteriores; F, fémur; Fi, fíbula; Fp, falanges extremidades anteriores; i, central; Mc, metacarpales; Mt, metatarsales; p, epífisis proximal; r, radial; Ra, radio; u, ulnar; Ul, ulna; Td III, IV, tarsales distales 3 y 4; Ti, tibia. Los eventos sin p o d incluyen los dos extremos del hueso.

Table 3 (cont.). Ossification sequences in the skeleton of *Anadia bogotensis, Riama striata, Bachia bicolor* and *Alopoglossus bicolor*. Abbreviations for events: Cf, complete fusion; S, separate; Sc, secondary center of ossification; Sf, fusing and suture present. Abbreviations for skull: Bo, basioccipital; Bs, sphenoid; Eo, exoccipital; Fr-co, frontal complete ossification; Fr-io, frontal incomplete ossification; P-co, parietal complete ossification; P-io, parietal incomplete ossification; Pro, prootic; Ot, otoccipital; So, supraoccipital. Abbreviations for limbs: Ast+Cal, astragalus and calcaneum; Cd I, II, III, IV, V, distal carpals 1-5; d, distal epiphyseal cartilages; H, humerus; Hp, hindlimb phalangeal cartilages; F, femur; Fi, fíbula; Fp, forelimb phalanges; i, centrale; Mc, metacarpals; Mt, metatarsals; p, proximal epiphyseal cartilages; r, radiale; Ra, radius; u, ulnare; Ul, ulna; Td III, IV, distal tarsals 3 and 4; Ti, tibia. The events without p or d refers both.

Species	Rank	Skull	Limbs
B. bicolor	1	Fr-io, P-io, Bo+Bs S, So+Eo S, Ot Cf, Ot+Bo S, Pro+Ot S, Pro+Bs S	
	2		H Sc, Ul Sc, Mc Sc, p Fp Sc, r, u, Cd III y IV, d F Sc
	3		Ra Sc, i, p F Sc
	4	Fr-co, P-co	
	5		F Sf
	6		d Mc Cf, p Fp Cf
	7	Bo+Bs Cf, So+Eo Cf, Ot+Bo Cf, Pro+Ot Cf, Pro+Bs Cf	H Sf, d Ra Sf, Ul Sf, p Mc Sf, F Cf
	8		H Cf, p Ra Sf, d Ra Cf, Ul Cf, p Mc Cf
	9		p Ra Cf
A. bicolor	1	Fr-io, P-io, Bo+Bs S, So+Eo S, Ot S, Ot+Bo S, Pro+Ot S, Pro+Bs S	H Sc, d Ra Sc, Ul Sc, Mc Sc, p Fp Sc, i, r, u, Cd II, III, IV, y V, F Sc, d Ti Sc, d Fi Sc, Mt Sc, p Hp Sc, Ast+Cal S, Td III, Td IV
	2		p Fi Sc
	3	Ot Sf	
	4	Ot Cf, Ot+Bo Sf, Pro+Bs Sf	H Sf, Ra Sf, Ul Sf, p Mc Cf, d Mc Sf, p Fp Sf, F Sf, Ti Sf, Fi Sf, Mt Sf, p Hp Sf, Ast+Cal Cf
	5	Fr-co, P-co, So+Eo Sf, Pro+Ot Sf	
	6	So+Eo Cf, Ot+Bo Cf, Pro+Ot Cf, Pro+Bs Cf	H Cf, Ul Cf, d Mc Cf, p Fp Cf, p F Cf, Mt Cf, p Hp Cf
	7		d Ra Cf, d F Cf, Ti Cf, Fi Cf
	8	Bo+Bs Cf	p Ra Cf

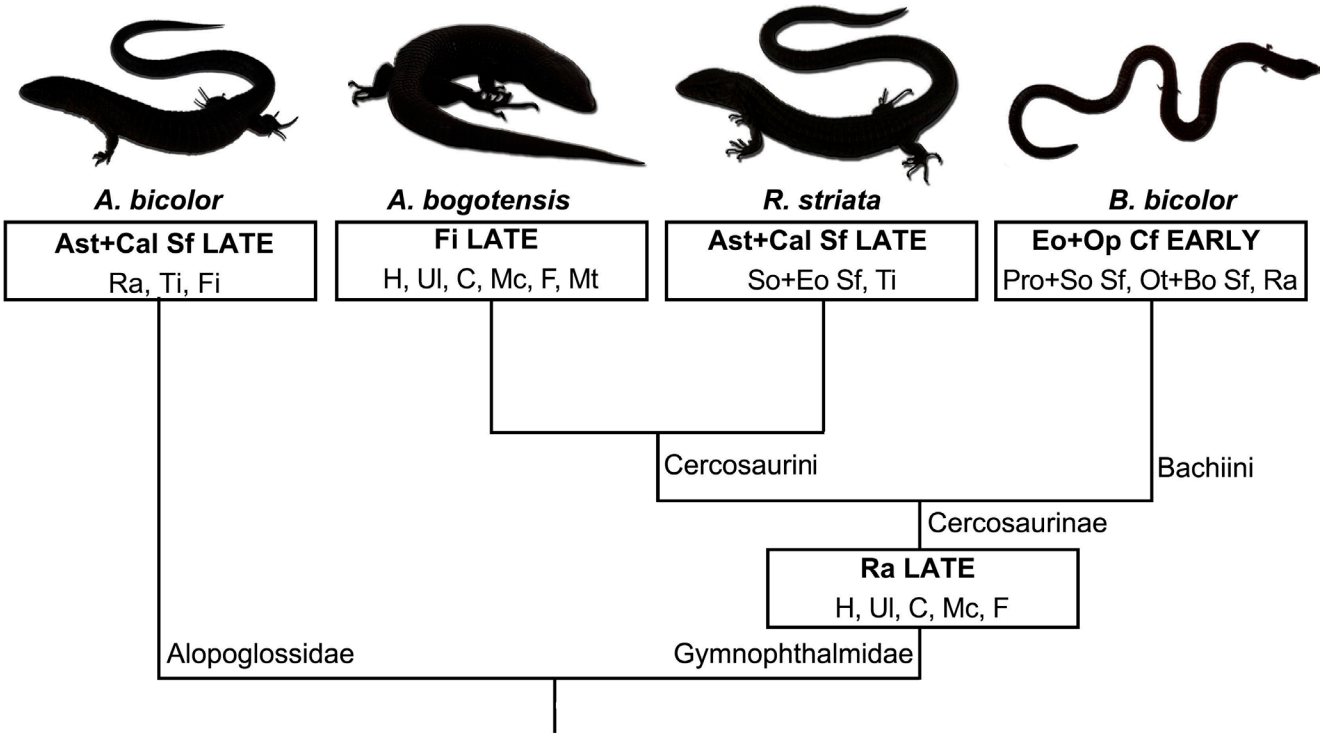

Figura 7. Eventos heterocrónicos con base en el algoritmo de parsimonia en la filogenia de Gymnophthalmoidea (Goicoechea et al., 2016).

Figure 7. Heterochronic events based on parsimony algorithm within the phylogeny established for Gymnophthalmoidea (Goicoechea et al., 2016).

in the neonate closes in small to medium-sized adults, after sexual maturity is reached. This pattern is shared by other gymnophthalmids such as *Potamites ecpleopus* (Bell et al., 2003), and the serpentiform Gymnophthalminae *Calyptommatus sinebrachiatus* and *Nothobachia ablephara* (Roscito & Rodrigues, 2012b). In Teiidae, the frontoparietal fontanelle is present in neonates of *Aspidocelis tigris*, *Cnemidophorus lemniscatus*, *Salvator merianae* and *Salvator rufescens* (Arias & Lobo, 2006), and it probably closes in small to medium-sized adults (Maisano, 2001).

This means, Gymnophthalmoidea exhibits the pattern described by Maisano (2001) for lizards that do not belong to the Iguania clade, in which the frontoparietal fontanelle closes in small to medium-sized adults and before the fusion of the elements of the basicranium. Furthermore, it occurs earlier than in lizards from the Iguania clade, such as Phrynosomatidae and Tropiduridae, in which it closes in very large adults (Maisano, 2002a; Torres-Carvajal, 2003).

In Squamata, basicranium ossification begins during embryonic development; then, neonates exhibit all elements ossified separated by synchondrosis, except for the sphenoid and basioccipital which are not completely ossified, and the basicranial fenestra is present; finally, all elements fuse in adults (Bellaris & Kamal, 1981; Maisano, 2002a, b). Neonates of *A. bogotensis*, *R. striata* and *A. bicolor* share this pattern with *B. bicolor*, *P. ecpleopus*, *A. tigris* and probably with *N. ablephara* and *C. sinebrachiatus* (Maisano, 2001; Tarazona et al., 2008; Roscito & Rodrigues, 2012b). This show that this pattern is shared by Gymnophthalmoidea.

In *A. bogotensis*, *R. striata*, and *A. bicolor*, the first elements to begin fusion are the exoccipital with the opisthotic to form the otoccipital in juveniles, and fusing completely in adults; while, in *B. bicolor*, *P. ecpleopus* and *A. tigris*, the otoccipital was reported in neonates (Maisano, 2001; Tarazona et al., 2008), and in *C. sinebrachiatus* it was observed in prenatal embryos (Roscito & Rodrigues, 2012b). Maisano (2001) found that the fusion of the exoccipital with the opisthotic in general in Squamata begins in embryonic stages and is complete in neonates, but there are exceptions like xantusids, *Lacerta* species and *Lanthanotus borneensis*. This evidence reveals that this event presents a high variation in Gymnophthalmoidea and Squamata.

Limbs

In the forelimbs, *A. bogotensis*, *R. striata*, *B. bicolor*, and *A. bicolor* share events related to the initiation of ossifications in neonates, with SCs in humeral, ulnar, and distal metacarpal epiphyseal cartilages, and OCs in the carpus. This pattern is also shared by *P. ecpleopus* and *A. tigris* (Maisano, 2001). Even *N. ablephara*, which exhibits only one-digit, presents SCs in distal humeral and metacarpal IV epiphyseal cartilages and OCs in distal carpal 5 in late embryos (Roscito & Rodrigues, 2012a, b). Arias & Lobo (2006) reported SCs in the forelimb at the end of embryonic development in *S. rufescens*, but not in *S. merianae*. In Gymnophthalmoidea neonates exhibit ossification centers in almost all epiphyses and distal carpal elements of the forelimb, as reported by Maisano (2001) for Squamata in general.

For the carpus, Fabrezi et al. (2007) found that the lizard carpus exhibits few variation (e.g., absence of distal carpal 1), since it is subject to strong developmental constraints. This element is variably present in families of Gymnophthalmoidea; the alopoglossid *A. bicolor* does not present this element, but the teiids *S. rufescens* and *S. merianae* exhibit a complete carpus (Arias & Lobo, 2006). In Gymnophthalmidae, distal carpal 1 is absent in the species of subfamily Gymnophthalminae like *Procellosaurinus tetradactylus*, *Vanzosaura rubricauda*, *Psilops paeminosus*, *N. ablephara*, *C. sinebrachiatus*, and *Scriptosaura catimbau* (Roscito & Rodrigues, 2012b; 2013; Roscito et al., 2014). In Cercosaurinae, *A. bogotensis* and *R. striata* exhibit a complete carpus, although distal carpal 1 is one of the last elements to ossify; but in species such as *B. bicolor*, tribe Bachini, it is absent (Jerez & Tarazona, 2009). It has been proposed that there are heterochronic mechanisms such as hypomorphosis (paedomorphosis) involved in limb reductions in Gymnophthalmidae (Jerez et al., 2020). Furthermore, there may be a difference in expression of sonic hedgehog in this species since, in *C. sinebrachiatus*, the development of the forelimb is arrested in the absence of sonic hedgehog expression, whereas continuous expression occurs in the hindlimb (Roscito et al., 2014). This should be evaluated in a comparative analysis using more species of Gymnopthalmoidea.

In the hindlimbs, neonates of *A. bogotensis*, *R. striata*, and *A. bicolor* exhibit SCs in proximal femoral, fibular, distal metatarsals, and phalangeal epiphyseal cartilage, and OCs in the tarsus. This pattern is the same in neonates of *P. ecpleopus* and *A. tigris* (Maisano, 2001). However, in serpentiform lizards, ossifications vary with the degree of reduction, so that in the hindlimb of *C. sinebrachiatus* with one digit, and *N. ablephara* with two digits, prenatal embryos exhibit ossifications in some epiphyses and tarsal elements (Roscito & Rodrigues, 2012b; Roscito et al., 2014). The neonate of *B. bicolor* only exhibits ossifications in the distal femoral epiphyseal cartilage, while the other epiphyseal cartilages and tarsal elements are cartilaginous (Jerez & Tarazona, 2009). This implies that neonates of Gymnophthalmoidea show high rate of ossifications in the hindlimb; however, the development of *B. bicolor* ossifications is delayed with respect to the rest of the studied species within Gymnophthalmoidea, indicating that reductions are not only evident during embryologic development of cartilages, but also in the ossifications during postnatal development.

Maisano (2002a, b) reported that Squamata exhibit a limb pattern of ossification in which the stylopodium ossifies before the zeugopodium, with the radius and tibia being the last elements to ossify. The gymnophthalmids analyzed show greater ossification development in the proximodistal and postaxial axis in neonates, thus the radius and tibia of *A. bogotensis*, *R. striata*, and *B. bicolor* develop SCs from juvenile to adult stages. In *A. bicolor* the radius and tibia develop SCs in the neonatal stage, as does the teiid *A. tigris* (Maisano, 2001). Gymnophthalmidae shows a late development of SCs in the radial and tibial epiphyses, compared to Alopoglossidae and Teiidae. Hence, Gymnophthalmidae exhibits a heterochronic event related to the radius since their epiphyseal cartilages develop SCs later than humeral, ulnar, metacarpals and femoral epiphyseal cartilages, and OCs in the carpus (Fig. 6). This highlights the importance of ossification patterns and morphological information in the evolution of Squamates.

In Squamata, the epiphyseal ossification starts with the development of SCs in the limbs. Later, epiphyseal cartilages ossify, but maintain a suture with the diaphyses. This event was observed in small to medium-sized adults in *A. bogotensis*, *R. striata*, *A. bicolor*, and *B. bicolor*. Finally, the complete fusion is observed in adults. This pattern was supported in Gymnophthalmoidea by the rank analysis (Fig. 6); and it was observed by Maisano (2002a, b, c) in Xanthusidae and Phrynosomatidae and probably, this is a pattern shared by Squamata.

In the limbs, the gymnophthalmids *A. bogotensis* and *R. striata* retain some epiphyses with the suture in large adults, and they continue to grow, as the growth plate is probably active since the suture is observed in distal femoral, ulnar/fibular, radial/tibial, and some phalangeal epiphyses (Haines, 1969; Andrews, 1982). Calderón-Espinosa et al. (2018) found that *A. bogotensis* has a moderate to high growth rate from birth to sexual maturity, then decreases, but individuals continue to grow until they die at about two years of age. This growth pattern could be shared by *R. striata*, as the two species have the same pattern in the

epiphyses, and they inhabit between 2000 m to 4000 m in the highland Andean ecosystem (Jerez & Calderón-Espinosa, 2014; Méndez-Galeano & Pinto-Erazo, 2018). This contrast with *A. bicolor*, *B. bicolor* and, *C. lemniscatus* which inhabit below 1500 m (Jerez & Tarazona, 2009; Ramos-Pallares et al., 2010; Uetz et al., 2021). Life history arise as an essential factor to consider in understanding the phylogenetic basis of ossification patterns, which has also observed by Maisano (2001) in differences in the state of ossification in neonates between viviparous and oviparous species.

Sesamoids

Sesamoids are elements in tendons, ligaments, between bones, and within joints (Haines, 1969; Jerez et al., 2010; Abdala et al., 2019). A functional origin has been hypothesized due to biomechanical effects since they strengthen the tendon under pressure and offer a mechanical advantage to the respective muscle (Nussbaum, 1982; Sarin et al., 1999; Abdala et al., 2019). However, some sesamoids develop late in the embryo or the neonate and are shared by almost all families of Squamata, indicating a phylogenetic factor involved in their presence (Maisano, 2002a; Jerez et al., 2010). *A. bogotensis*, *R. striata*, and *A. bicolor* share some sesamoids during ontogeny (Table 2), commonly present in Squamata, such as the pisiform, tibial lunula, dorsal preaxial lunula, tibial patella, palmar sesamoid, plantar sesamoid, ulnar patella, distal phalangeal sesamoid in the manus and pes, fabella, parafibula, and ventral preaxial tarsal sesamoid (Jerez et al., 2010). Some of these are also present in adults of other species such as *Cercosaura schreibersii*, *Loxopholis rugiceps*, *Loxopholis southi*, *Pholidobolus montium*, *Cercosaura argulus*, *Pholidobolus vertebralis*, *Tretioscincus bifasciatus*, *Alopoglossus stenolepis*, *Kentropyx viridistriga*, and *C. lemniscatus* (Jerez et al., 2010; Otero & Hoyos, 2013).

Serpentiform species such as *B. bicolor* only develop the pisiform and palmar sesamoid. This reduction is observed in the limb-reduced skink *Chalcides*, which only develops the pisiform, palmar sesamoid, plantar sesamoid, tibial lunula, and the dorsal preaxial tibiofemoral lunula (Jerez et al., 2010); in both cases, they present common sesamoids in lizards, which develop from embryonic stages (Jerez et al., 2010), and therefore, the reductions impact their development.

The pattern of sesamoid development during ontogeny observed in *A. bogotensis*, *R. striata*, and *A. bicolor* shows that other sesamoids develop in postembryonic stages, and that they are variable among Squamata (Jerez et al., 2010). Therefore, the sesamoids that develop postnatally do so as a response to mechanical stress and constitute highly variable elements (Abdala et al., 2019; Fontanarrosa et al., 2020).

Apophyseal ossifications

The apophyseal ossifications are independent mineralization of metaplastic origin, which appear at the insertion of tendons and ligaments (Haines, 1969). The region where the tendon is inserted into the bone is known as the enthesis or tendon-bone transition and is a zone of concentration of mechanical stress such as compression-tension forces (Gao et al., 1996). In lizards, the apophyseal ossifications of the enthesis are observed in juveniles and disappear in adults (Maisano 2002a, b), a pattern shared by *A. bogotensis*, *R. striata*, *A. bicolor*, and *B. bicolor*. In mammals, the enthesis responds to the post-embryonic development of the musculoskeletal system and adjusts to the growth of the bones and biomechanical needs that arise after birth, and this is achieved by processes of osteoclastic reabsorption and simultaneous osteogenic activity (Wei & Messner, 1996). Probably, these processes are involved in the development of apophyseal ossifications in Squamata, but histological studies are necessary.

CONCLUSIONS

Postnatal ossification patterns of *A. bogotensis*, *R. striata*, and *B. bicolor* share characteristics with other squamates. For the dermatocranium, the frontoparietal fontanelle closes in small to medium-sized adults, before the fusion of the elements of the basicranium. For the chondocranium, the ossification begins in embryonic stages; the neonates exhibit all elements ossified separated by synchondrosis but the basicranial fenestra is present, and all elements fuse in adults. In appendicular skeleton, the neonates exhibit SCs in almost all epiphyses and OCs in distal carpal/tarsal elements. The epiphyseal ossification starts with the development of SCs in neonates; epiphyseal cartilages ossify, but maintain a suture with the diaphysis in small to medium-sized adults and the complete fusion is observed in adults. On the other hand, Gymnophthalmidae exhibits a heterochronic event, the radial epiphyseal cartilages develop SCs later than the epiphyseal cartilages of the humerus, ulna, metacarpals and femur, and OCs in the carpus. In the future, with more information from Alopoglossidae, Teiidae, and Gymnophthalmidae, we will be able to corroborate several of the patterns of Squamata ossification and determine heterochronies for the whole clade and families.

Acknowledgments.— We would like to thank Alejandra Arias for her participation in obtaining the data for *R. striata*; also, to Laboratorio de Equipos Ópticos Compartidos (LEOC), Departamento de Biología, Universidad Nacional de Colombia,

sede Bogotá. We also thank Martha Calderón-Espinosa, curator of the Colección de Reptiles (Instituto de Ciencias Naturales, Universidad Nacional de Colombia, sede Bogotá) and Martha Patricia Ramírez, curator of the Colección Herpetológica (Universidad Industrial de Santander), for the loan of the specimens of *A. bogotensis* and *R. striata*. Also, to Stephane Bryant and Juliana A. Rodríguez F. by reviewing the english writing, and the reviewers, whose comments improved this manuscript.

CITED LITERATURE

Abdala, V., M.C. Vera, L.I. Amador, G. Fontanarrosa, J. Fratani, & M.L. Ponssa. 2019. Sesamoids in tetrapods: the origin of new skeletal morphologies. Biological Reviews 94:2011-2032.

Andrews, R.M. 1982. Patterns of growth in reptiles. Pp. 273-320. In Gans C & Pough FH (Eds.), Biology of the Reptilia Vol 13. Academic Press.

Arias, F. & F. Lobo. 2006. Patrones de osificación en *Tupinambis merianae* y *Tupinambis rufescens* (Squamata: Teiidae) y patrones generales en Squamata. Cuadernos de Herpetología 20:3-23.

Barros, F.C., A. Herrel & T. Kohlsdorf. 2011. Head shape evolution in Gymnophthalmidae: does habitat use constrain the evolution of cranial design in fossorial lizards? Journal of Evolutionary Biology 24:2423–2433.

Bell, C.J., S.E. Evans & J.A. Maisano. 2003. The skull of the gymnophthalmid lizard *Neusticurus ecpleopus* (Reptilia: Squamata). Zoological Journal of the Linnean Society 139:283-304.

Bellairs, A.D. & A.M. Kamal. 1981. The chondrocranium and the development of the skull in recent reptiles. Pp. 1-283. In C. Gans & T.S. Parsons (Eds.), Biology of the Reptilia: morphology. Academic Press, New York, USA.

Calderón-Espinosa, M., A. Ramírez & A. Jerez. 2018. Growth pattern of the tropical highland gymnophthalmid lizard *Anadia bogotensis* in captivity conditions. Acta Biológica Colombiana 23:307-310.

Castoe, T.A., T.M. Doan & C.L. Parkinson. 2004. Data partitions and complex models in Bayesian analysis: the phylogeny of gymnophthalmid lizards. Systematic Biology 53:448–469.

Estes, R., K. de Queiroz & J. Gauthier. 1998. Phylogenetic relationships within Squamata. Pp. 119-281. In R. Estes & G. Pregill (Eds.), Phylogenetic Relationships of the Lizard Families. Stanford University Press, Stanford, California.

Evans, S.E. 2008. The skull of lizards and Tuatara. Morphology H. The skull of Lepidosauria. Pp. 1-347. In C. Gans & T.S. Parsons (Eds), Biology of the Reptilia: morphology. Academic Press, New York, USA.

Fabrezi, M., V. Abdala & M.I. Martínez. 2007. Developmental basis of limb homology in lizards. The Anatomical Record 290:900-912.

Fontanarrosa, G., J. Fratani & M.C. Vera. 2020. Delimiting the boundaries of sesamoid identities under the network theory framework. Peer J 8:e9691.

Gao, J., K. Messner, J.R. Ralphs & M. Benjamin.1996. An immunohistochemical study of enthesis development in the medial collateral ligament of the rat knee joint. Anatomy and Embryology 194:399-406.

Germain, D. & M. Laurin. 2009. Evolution of ossification sequences in salamanders and urodele origins assessed through event-pairing and new methods. Evolutionary Development 11:170-190.

Goicoechea, N., D.R. Frost, I. De la Riva, K.C.M Pellegrino, J.W. Sites, M.T. Rodrigues & J.M. Padial. 2016. Molecular systematics of teiid lizards (Teiioidea/Gymnophthalmoidea: Squamata) based on the analysis of 48 loci under tree-alignment and similarity-alignment. Cladistics 32:624-671.

Greer, A.E. 1991. Limb reduction in Squamates: identification of the lineages and discussion of the trends. Journal of Herpetology 25:166-173.

Grizante, M.B., R. Brandt & T. Kohlsdorf. 2012. Evolution of body elongation in Gymnophthalmid lizards: relationships with climate. PloS One 7:e49772.

Haines, R.W. 1969. Epiphyses and sesamoids. Pp. 81-122. In Gans, C., A. Bellairs & T. S. Parsons (Eds.). Biology of the Reptilia, Vol. 1. Morphology A. Academic Press, London, England.

Hautier, L., N.C. Bennett, H. Viljoen, L. Howard, M.C. Milinkvitch, A. Tzika, A. Goswami & R. Asher. 2013. Patterns of ossification in southern versus northern placental mammals. Evolution 67:1994-2010.

Hernández-Jaimes, C., A. Jerez & M.P. Ramírez-Pinilla. 2012.

Embryonic development of the skull of the Andean lizard *Ptychoglossus bicolor* (Squamata, Gymnophthalmidae). Journal of Anatomy 221:285-302.

Hernández-Morales, C., P.L. Peloso, W. Bolívar & J.D. Daza. 2019. Skull morphology of the lizard *Ptychoglossus vallensis* (Squamata: Alopoglossidae) with comments on the variation within Gymnophthalmoidea. The Anatomical Record 302:1074-1092.

Hoyos, J.M. 1998. A reappraisal of the phylogeny of lizards of the family Gymnophthalmidae (Sauria, Scincomorpha). Revista Española de Herpetología 12:27-43.

Jeffery, J.E., O.R.P. Bininda-Emonds, M.I. Coates & M.K. Richardson. (2005). A new technique for identifying sequence heterochrony. Systematic Biology 54:230-240.

Jerez, A. & O.A. Tarazona. 2009. Appendicular skeleton in *Bachia bicolor* (Squamata: Gymnophthalmidae): osteology, limb reduction and postnatal skeletal ontogeny. Acta Zoologica 90:42-50.

Jerez, A., S. Mangione & V. Abdala. 2010. Occurrence and distribution of sesamoid bones in squamates: A comparative approach. Acta Zoologica 91:295-305.

Jerez, A. & M. Calderón-Espinosa. 2014. *Anadia bogotensis* (Peters, 1862). Lagartija Anadia de Bogotá. Catálogo de Anfibios y Reptiles de Colombia 2:30-35.

Jerez, A., A. Bonilla-Garzón & S. Castellanos. 2020. Estados de desarrollo en *Anadia bogotensis*: aportes a la comprensión de la evolución del plan corporal en Gymnophthalmoidea (Squamata). Cuadernos de Herpetología 34:1-12.

Keyte, A.L. & K.K. Smith. 2010. Developmental origins of precocial forelimbs in marsupial neonates. Development 137:4283-4294.

Koyabu D. & N.T. Son. 2014. Patterns of postcranial ossification and sequence heterochrony in bats: Life histories and developmental trade-offs. Journal of Experimental Zoology Part B: Molecular and Developmental Evolution 322(8):607-618.

Kohlsdorf, T. & G.P. Wagner. 2006. Evidence for the reversibility of digit loss: a phylogenetic study of limb evolution in *Bachia* (Gymnophthalmidae: Squamata). Evolution 60:1896-1912.

Krause, L. 1989. Morfologia e aspectos funcionais doesqueleto apendicular de macroteiídeos (Sauria, Scincomorpha, Teiidae). Boletim do Instituto de Biociencias 47:9-113.

Lungman, J.L., M.N. Molinero, M.S. Simoncini & C.L. Piña. 2019. Embryological development of *Salvator merianae* (Squamata: Teiidae). Genesis 57: e23280.

Maisano, J.A. 2001. A survey of state of ossification in neonatal squamates. Herpetological Monographs 15:135-37.

Maisano, J.A. 2002a. The potential utility of postnatal skeletal developmental patterns in squamate phylogenetics. Zoological Journal of the Linnean Society 136:277-313.

Maisano, J.A. 2002b. Postnatal skeletal ontogeny in *Callisaurus draconoides* and *Uta stansburiana* (Iguania: Phrynosomatidae). Journal of Morphology 251:114-139.

Maisano, J.A. 2002c. Postnatal skeletal ontogeny in five xantusiids (Squamata: Scleroglossa). Journal of Morphology 254:1-38.

Méndez-Galeano, M.A. & M.A. Pinto-Erazo. 2018. *Riama striata* (Peters 1863). Lagartija estriada. Catálogo de Anfibios y Reptiles de Colombia 4:61-67

Nunn, C.L. & K.K. Smith. 1998. Statistical analyses of developmental sequences: the craniofacial region in marsupial and placental mammals. American Naturalist 152:82-101.

Nussbaum, R.A. 1982. Heterotopic bones in the hind limbs of frogs of the families Pipidae, Ranidae, and Sooglossidae. Herpetologica 38:312-320.

Otero, T. & J.M. Hoyos. 2013. Sesamoid elements in lizards. Herpetological Journal 23:105-114.

Pellegrino, K.C.M., M.T. Rodrigues, Y. Yonenaga-Yassuda & J.W. Sites. 2001. A molecular perspective on the evolution of microteiid lizards (Squamata, Gymnophthalmidae), and a new classification for the family. Biological Journal of the Linnean Society 74:315-38.

Presch, W.F. 1975. The evolution of limb reduction in Teiid lizard genus *Bachia*. Bulletin of the Southern California Academy of Sciences 74:113-121.

Presch, W.F. 1980. Evolutionary history of the South American microteiid lizards (Teiidae: Gymnophthalminae). Copeia 1980:36-56.

Presch, W.F. 1983. The lizard family Teiidae: is it a monophyletic

group?. Zoological Journal of the Linnean Society 77:189-197.

Ramos-Pallares, E.P., V.H. Serrano-Cardozo & M.P. Ramírez-Pinilla. 2010. Reproduction of *Ptychoglossus bicolor* (Squamata: Gymnophthalmidae) in an Andean coffee shade plantation in Colombia. South American Journal of Herpetology 5:143-150.

Roscito, J.G. & M.T. Rodrigues. 2012a. Embryonic development of the fossorial gymnophthalmid lizards *Nothobachia ablephara* and *Calyptommatus sinebrachiatus*. Zoology 115:302-318.

Roscito, J.G. & M.T Rodrigues. 2012b. Skeletal development in the fossorial lizards *Nothobachia ablephara* and *Calyptommatus sinebrachiatus*. Zoology 115:289-301.

Roscito, J.G. & M.T. Rodrigues. 2013. A comparative analysis of the post-cranial skeleton of fossorial and non-fossorial gymnophthalmid lizards. Journal of Morphology 274:845-858.

Roscito, J.G., P.M. Nunes & M.T. Rodrigues. 2014. Digit evolution in gymnophthalmid lizards. The International Journal of Developmental Biology 58:895-908.

Sarin, V.K., G.M. Erickson, N.J. Giori, A.G. Bergman & D.R. Carter. 1999. Coincident development of sesamoid bones and clues to their evolution. The Anatomical Record 257:174-180.

Smith, K.K. 2001. Heterochrony revisited: the evolution of developmental sequences. Biological Journal of the Linnean Society 73:169-186.

Tarazona O.A., M. Fabrezi & M.P. Ramírez-Pinilla. 2008. Cranial morphology of *Bachia bicolor* (Squamata: Gymnophthalmidae) and its postnatal development. Zoological Journal of the Linnean Society 152:775-792.

Torres-Carvajal, O. 2003. Cranial osteology of the Andean lizard *Stenocercus guentheri* (Squamata:Tropiduridae) and its postembryonic development. Journal of morphology 255:94-113.

Uetz, P., P. Freed & J. Hošek (Eds.). 2021. The Reptile Database. http://www.reptile-database.org, [Accessed on 22 June 2021]

Wassersug, R.J. 1976. A procedure for differential staining of cartilage and bone in whole formalin fixed vertebrates. Stain Technology 51:131-134.

Wei, X. & C. Messner. 1996. The postnatal development of the insertions of the medial collateral ligament in the rat knee. Anatomy and Embryology 193:53-59.

Werneburg, I. 2009. A standard system to study vertebrate embryos. PloS One 4:e5887

APPENDIX 1.

Anadia bogotensis (ICN): Colección de Reptiles, Instituto de Ciencias Naturales, Universidad Nacional de Colombia, sede Bogotá (Bogotá-Colombia). Neonates: ICN 13433, 23.86 mm SVL; ICN 13434, 22.33 mm SVL; ICN 13435: 26.46 mm SVL. Juveniles: ICN 13436, 31.36 mm SVL; ICN 9884, 36.55 mm SVL. Adults: ICN 4534, 42.53 mm SVL; ICN 9865, 48.63 mm SVL; ICN 13437, 50.36 mm SVL; ICN 13438, 50 mm SVL; ICN 13439, 52.6 mm SVL; ICN 9866, 58.23 mm SVL; ICN 9861, 62.67 mm SVL.

Riama striata (ICN): Colección de Reptiles, Instituto de Ciencias Naturales, Universidad Nacional de Colombia, sede Bogotá (Bogotá, Colombia). Neonates: ICN 13440, 28 mm SVL; ICN 13441, 28.85 mm SVL. Juveniles: ICN 13442, 38.7 mm SVL. Adults: ICN 13443, 52.63 mm SVL; ICN 13444, 58.02 mm SVL; ICN 13445, 66.22 mm SVL.

Alopoglossus bicolor (UIS-R): Colección Herpetológica, Escuela de Biología, Universidad Industrial de Santander (Bucaramanga, Colombia). Neonates: UIS-R 2578, 23.8 mm SVL; UIS-R 2580, 20.2 BL. Juveniles: UIS-R 2596, 30.24 mm SVL; UIS-R 2595, 43.88 mm SVL; UIS-R 2583, 44.28 mm SVL. Adults: UIS-R 1550, 50.24 mm SVL; UIS-R 2584, 51.46 mm SVL; UIS-R 1540, 51.92 mm SVL; UIS-R 1575, 53.58 mm SVL; UIS-R 1579, 54.4 mm SVL; UIS-R 1590, 55.12 mm SVL; UIS-R 1560, 56.24 mm SVL; UIS-R 2594, 60.28 mm SVL.